

## 7.1 Introduction

Oral bioavailability depends on a number of factors including drug's aqueous solubility, dissolution rate, drug permeability, first pass metabolism and intestinal efflux. The *in-vitro* tests do not represent the true physiological environment and hence not able to predict the true pharmacokinetics of the drug. Moreover, in case of nano-sized systems, the effect of particulate uptake on oral bioavailability cannot be predicted by *in-vitro* characterization. Therefore, in order to predict more accurate bioavailability, *in-vivo* pharmacokinetic studies need to be carried out. Since, the absorption of drug/nanoparticles uptake could be different in stomach and intestine due to their physiological differences, the *in-situ* absorption studies from stomach and intestine are helpful in understanding the absorption site upon administration of drug loaded nanoparticles. Moreover, the lipid based drug delivery systems increases the lymphatic absorption of drug and hence, the biodistribution pattern upon administration of lipid nanoparticles/nanoemulsion was estimated in various organs. The biodistribution of nanoparticles in peyer's patch and non-peyer's patch was also estimated to verify the difference in uptake of nanoparticles in these regions since peyer's patches are a part of lymphoid follicle system and direct the lymphatic absorption of particulate systems.

## 7.2 Materials

Cycloheximide was procured from HiMedia laboratories, India. Acetonitrile was purchased from Spectrochem (Mumbai, India). Acetic acid, sodium chloride, potassium chloride and calcium chloride were procured from SD Fine chemicals, India.

## 7.3 Animals

For various *in-vivo* studies, male wistar rats weighing  $250 \pm 20$  g were used. The animals (3 rats per cage) were housed in propylene cages (38 cm x 23 cm x 10 cm) in animal room at temperature 20-25°C. Artificial lighting with the sequence of 12 hr light and 12 hr dark was kept in animal housing. For feeding, conventional rodent laboratory diet was used with an unlimited supply of drinking water. All experiments and protocols described in this study were approved by the Institutional Animal Ethics Committee of

The M.S. University of Baroda and were in accordance with guidelines of the committee for purpose of control and supervision of experiments on animals (CPCSEA), ministry of social justice and empowerment, Government of India (Protocol no: MSU/PHARM/IAEC/2011/29).

## **7.4 Methods**

### **7.4.1 *In-vivo* methods of Darunavir loaded solid lipid nanoparticles**

#### **7.4.1.1 Pharmacokinetic profile comparison of three different sized- Darunavir loaded solid lipid nanoparticles**

The pharmacokinetic behavior of SLNs (all three sizes), plain drug suspension and marketed tablet (DARUVIR-300 mg tablet) was investigated in rats after single oral dose administration. The wistar rats were fasted overnight with free access to water and randomly divided into 6 groups (n=3). The 1<sup>st</sup> group was given saline (negative control), 2<sup>nd</sup> group was given Darunavir suspension (40mg/kg) prepared using 0.4 % w/v methyl cellulose, 3<sup>rd</sup> group was given marketed tablet preparation (powdered tablet and suspended in distilled water), 4<sup>th</sup> group was given Dar-SLN1, 5<sup>th</sup> group was given Dar-SLN2 and 6<sup>th</sup> group was given Dar-SLN3 (lyophilized form of nanoparticles were suspended in distilled water before administration). The formulations were administered orally with the aid of syringe and infant feeding tube at the dose of 40mg/kg (1, 2). 0.4 ml Blood samples were drawn by retro-orbital venous plexus puncture with the aid of capillary tubes at predose, 0.5, 1, 2, 4, 8 and 24 hr post oral dose. The samples were collected in heparinized eppendorf tubes and centrifuged at 5000 rpm for 15 min. The plasma was collected and stored at -20°C until analysis.

The samples were analyzed using developed LCMS method (Chapter 3). Acetonitrile was added to plasma sample in ratio of 4:1 (acetonitrile: plasma) and centrifuged to remove plasma proteins. The supernatant was taken and analyzed using LCMS. The individual plasma concentration-time profiles were subjected to non-compartmental model using Kinetica software (version 5.0.11, Thermofischer scientific). Peak plasma concentrations ( $C_{max}$ ), corresponding peak times ( $T_{max}$ ), half-lives ( $t_{1/2}$ ), MRT (mean residence time),  $AUC_{(0-t)}$  ( $AUC$  until last time point with measurable

plasma concentrations) and AUC<sub>(0-∞)</sub> values were calculated. AUCs were calculated by trapezoidal method using the kinetica software. Relative bioavailability was defined as percentage ratio between the AUC<sub>0-t</sub> values of SLNs and that of marketed formulation. Statistical analysis of data was performed using Student-t test. GraphPad Prism (version 5, USA) was used for all analyses and P value < 0.05 was considered significant.

#### **7.4.1.2 *In-situ* absorption from stomach and intestine**

The absorption of Darunavir suspension and optimized Darunavir loaded SLNs (Dar-SLN2) in gastro-intestinal tract (stomach and intestine) was investigated in rats by *in-situ* method (3). The animals were fasted overnight and anesthetized by intraperitoneal injection of Ketamine (50mg/kg). A small incision was made in abdomen and the pylorus of the stomach was ligated. SLNs were given to rats (40mg/kg) by intragastric administration to evaluate its absorption in stomach. Likewise, to measure the absorption of SLNs in the intestine, SLNs were intraduodenally administered to rats at the same dose (n=3). The incisions were stitched and rats were kept under infrared lamps to maintain body temperature. 0.4 ml blood sample was collected at 15, 30, 45, 60 and 90 min and plasma was separated by centrifugation at 3000 rpm for 15 min. 0.2 ml of supernatant was diluted to 1ml using chilled acetonitrile to precipitate plasma proteins, centrifuged at 5000 rpm, 4°C for 10 min and the amount of Darunavir in supernatant was measured using developed LCMS method.

#### **7.4.1.3 Lymphatic transport study**

To study the intestinal transport of solid lipid nanoparticles in rats, cycloheximide solution- 0.6mg/ml (3mg/kg) was intraperitoneally injected to inhibit the secretion of chylomicrons from the enterocytes. In the control group, an equal volume of saline was intraperitoneally administered to rats. At 1 hr after the injection, rats were anesthetized and SLNs were intraduodenally administered to rats (40mg/kg), blood samples were drawn by retro-orbital venous plexus puncture with the aid of capillary tubes at predetermined time intervals. The samples were collected in heparinized eppendorf tubes and centrifuged at 5000 rpm for 15 min, and plasma was collected. 0.2 ml of supernatant was diluted to 1ml using chilled acetonitrile to precipitate plasma proteins, centrifuged at

5000 rpm, 4°C for 10 min and the amount of Darunavir in supernatant was measured using developed LCMS method.

#### **7.4.1.4 Organ biodistribution study**

For biodistribution studies, male wistar rats (weighing 250 ±20g) were divided into 2 groups with 12 animals in each group. They were fasted overnight before administration of dose. 1<sup>st</sup> group was given Darunavir suspension, 2<sup>nd</sup> group was given Dar-SLN2, both at the drug dose of 40mg/kg. 3 animals of both groups were sacrificed at each time point 1, 4, 8, and 24 hr. The organs (spleen, liver, kidney, stomach, intestine, brain, heart and lung) were excised, isolated, washed with Ringer's solution and dried using tissue paper. Organs were stored at -80°C until assay (Ringer's solution was prepared by accurately adding 7.2 g sodium chloride, 0.37 g potassium chloride and 0.17 g calcium chloride in distilled water to make 1 L and pH adjusted to 7.3-7.4).

For estimation of drug in different organs, following procedure was followed: Various organs were, weighed and cut into small pieces. 1 g organ was homogenized individually using tissue homogenizer in double distilled water (10% homogenate concentration). In case of organs weighing less than 1 g, the whole organ was used. The homogenate was centrifuged at 5000 rpm for 15 min, acetonitrile was added to tissue homogenate (4:1- acetonitrile: homogenate) and centrifuged to remove plasma proteins. The supernatant was taken and analyzed using developed LCMS method.

#### **7.4.1.5 Biodistribution of SLNs in Peyer's patch (PP) and Non-peyer's (Non-PP) patch**

##### **A) Identification of peyer's patch (4)**

Initially, visual identification of peyer's patch was done. Test was performed in order to confirm identification of peyer's patches. The procedure followed is given below.

*Procedure:*

A male wistar rat was sacrificed and small intestine was isolated, washed with PBS and cut into sections. The intestine sections were cut open, blotted dry and placed on transparent surface. The sections were viewed for presence of peyer's patches and images were taken. The sections were placed into glass vials containing 20 ml of 10% v/v aqueous acetic acid and incubated overnight in refrigerator. Acetic acid was used as it enhanced the visualization of the lymphoid tissue. The following day, sections were removed, blotted dry and photographed to view the presence of peyer's patches.

## **B) Protocol for biodistribution of SLNs in PP and Non-PP**

The distribution of SLNs in Peyer's patch and non-peyer's patch was studied as per method described by Desai et al (5). For this, Dar-SLN2 was administered at the dose of 40mg/kg to 8 male wistar rats. Two animals were sacrificed at each time intervals (1, 4, 8, 24 hr) and intestine was isolated, washed with Ringer's solution and blotted using tissue paper. Peyer's patch and Non-peyer's patch region were differentiated visually and separated. The regions were weighed, separately homogenized, centrifuged at 5000 rpm for 15 min, acetonitrile was added to tissue homogenate (4:1- acetonitrile: homogenate) and centrifuged to remove plasma proteins. The supernatant was taken and analyzed using developed LCMS method.

### **7.4.2 *In-vivo* methods of optimized Peptide-grafted Darunavir loaded SLNs (Pept-Dar-SLN)**

#### **7.4.2.1 Pharmacokinetic study**

The peptide grafted SLNs loaded with Darunavir (Pept-Dar-SLN) were prepared as per procedure mentioned in section 4.3.2. Its pharmacokinetic behavior in male wistar rats was studied using same procedure as mentioned in section 7.4.1.1. The formulation was administered orally with the aid of syringe and infant feeding tube at the dose of 40mg/kg (n=3). 0.4 ml blood samples were drawn by retro-orbital venous plexus puncture with the aid of capillary tubes at 0.5, 1, 2, 4, 8 and 24 hr post oral dose. The samples were collected in heparinized eppendorf tubes and centrifuged at 5000 rpm for 15 min and filtered. The plasma was collected and stored at -20°C until analysis. The

samples were analyzed using developed LCMS method (Chapter 3). Acetonitrile was added to plasma sample in ratio of 4:1 (acetonitrile: plasma) and centrifuged to remove plasma proteins. The supernatant was taken and analyzed using LCMS. The plasma concentration-time profiles were subjected to non-compartmental model using Kinetica software (version 5.0.11, Thermofischer scientific) and various pharmacokinetic parameters were calculated.

#### **7.4.2.2 Organ biodistribution study**

For biodistribution studies of Pept-Dar-SLN, same procedure was followed as mentioned in 6.5.3. Male wistar rats (weighing 250 ±20g) were fasted overnight before administration of dose. Animals were given Pept-Dar-SLN at the drug dose of 40mg/kg. 3 animals were sacrificed at each time point 1, 4, 8, and 24 hr. The organs (spleen, liver, kidney, stomach intestine, brain, heart and lung) were excised, isolated, washed with Ringer's solution and dried using tissue paper. Organs were weighed and cut into small pieces. 1 g organ was homogenized individually using tissue homogenizer in double distilled water (10% homogenate concentration). In case of organs weighing less than 1 g, the whole organ was used. The homogenate was centrifuged at 5000 rpm for 15 min, acetonitrile was added to tissue homogenate (4:1- acetonitrile: homogenate) and centrifuged to remove plasma proteins. The supernatant was taken and analyzed using developed LCMS method.

#### **7.4.3 *In-vivo* methods of optimized Darunavir loaded Nanoemulsion (DNE-3)**

##### **7.4.3.1 Pharmacokinetic study**

The optimized Darunavir loaded nanoemulsion was prepared as per procedure mentioned in section 4.3.3.2. Its pharmacokinetic behavior in rats was studied using same procedure as mentioned in section 7.4.1.1. The male wistar rats were fasted overnight with free access to water and randomly divided into 2 groups (n=3). 1<sup>st</sup> group was given Darunavir loaded nanoemulsion (DNE-3) while 2<sup>nd</sup> group was given saline (control group). The formulation was administered orally with the aid of syringe and infant feeding tube at the dose of 40mg/kg (n=3) (1, 6). Blood samples were drawn by retro-

orbital venous plexus puncture with the aid of capillary tubes at predose, 0.5, 1, 2, 4, 8 and 24 hr post oral dose. The samples were collected in heparinized eppendorf tubes and centrifuged at 5000 rpm for 15 min and filtered. The plasma was collected and stored at -20°C until analysis. The samples were analyzed using developed LCMS method (Chapter 3). Acetonitrile was added to plasma sample in ratio of 4:1 (acetonitrile: plasma) and centrifuged to remove plasma proteins. The supernatant was taken and analyzed using LCMS. The plasma concentration-time profiles were subjected to non-compartmental model using Kinetica software (version 5.0.11, Thermofischer scientific) and various pharmacokinetic parameters were calculated.

#### **7.4.3.2 Organ biodistribution study**

Distribution of DNE-3 into various organs was studied as per procedure mentioned in section 7.4.1.4. 12 male wistar rats (weighing 250 ±20g) were used for the study. They were fasted overnight before administration of dose. Rats were given Darunavir loaded lipid nanoemulsion (at the drug dose of 40 mg/kg). 3 animals were sacrificed at each time point 1, 4, 8, and 24 hr. The organs (spleen, liver, kidney, stomach intestine, brain, heart and lung) were excised, isolated, washed with Ringer's solution and dried using tissue paper. The organs were weighed and cut into small pieces. 1 g organ was homogenized individually using tissue homogenizer in double distilled water (10% homogenate concentration). In case of organs weighing less than 1 g, the whole organ was used. The homogenate was centrifuged at 5000 rpm for 15 min, acetonitrile was added to tissue homogenate (4:1- acetonitrile: homogenate) and centrifuged to remove plasma proteins. The supernatant was taken and analyzed using developed LCMS method.

#### **7.4.4 *In-vivo* methods of optimized Peptide grafted Atazanavir sulfate loaded SLNs**

##### **7.4.4.1 Pharmacokinetic study**

The pharmacokinetic behavior of Atazanavir sulfate loaded solid lipid nanoparticles (ALN-23) and peptide grafted ATZ SLNs (Pept-ATZ-SLN) was studied in male wistar rats after single oral dose administration. The wistar rats were fasted

overnight with free access to water and randomly divided into 3 groups (n=3). The 1<sup>st</sup> group was given Pept-ATZ-SLN suspended in distilled water, 2<sup>nd</sup> group was given ALN23 suspended in distilled water and 3<sup>rd</sup> group was given plain drug suspension prepared using 0.4 % w/v methyl cellulose. The formulations were administered orally with the aid of syringe and infant feeding tube at the dose of 7 mg/kg (7). 0.4 ml blood samples were drawn by retro-orbital venous plexus puncture with the aid of capillary tubes at predetermined time intervals. The samples were collected in heparinized eppendorf tubes and centrifuged at 5000 rpm for 15 min and filtered. The plasma was collected and stored at -20°C until analysis.

The samples were analyzed using developed HPLC method (Chapter 3). Acetonitrile was added to plasma sample in ratio of 4:1 (acetonitrile: plasma) and centrifuged to remove plasma proteins. The supernatant was evaporated to dryness at room temperature and analyzed using HPLC after reconstitution with mobile phase (8). The individual plasma concentration-time profiles were subjected to non-compartmental model using Kinetica software (version 5.0.11, Thermofischer scientific) and various pharmacokinetic parameters were determined. Relative bioavailability was defined as percentage ratio between the AUC<sub>0-t</sub> value of ALN-23 and that of plain drug suspension.

#### **7.4.4.2 Organ biodistribution study**

Distribution of ATZ suspension, ATZ loaded solid lipid nanoparticles (ALN-23) and peptide grafted ATZ solid lipid nanoparticles (Pept-ATZ-SLN) into various organs was studied as per procedure mentioned in section 7.4.1.4. Male wistar rats (weighing 250 ±20g) were divided into 3 groups (12 animals in each group). They were fasted overnight before administration of dose. 1<sup>st</sup> group was given ATZ suspension (at the drug dose of 10 mg/kg) and 2<sup>nd</sup> group was given ALN-23 and 3<sup>rd</sup> group was given Pept-ATZ-SLN. 3 animals of each group were sacrificed at each time point 1, 2, 4, and 12 hr. The organs (spleen, liver, kidney, stomach intestine, brain, heart and lung) were excised, isolated, washed with Ringer's solution and dried using tissue paper. The organs were weighed and cut into small pieces. 1 g organ was homogenized individually using tissue homogenizer in double distilled water (10% homogenate concentration). In case of

organs weighing less than 1 g, the whole organ was used. The homogenate was centrifuged at 5000 rpm for 15 min, acetonitrile was added to tissue homogenate (4:1-acetonitrile: homogenate) and centrifuged to remove plasma proteins. The supernatant was taken and analyzed using developed HPLC method.

## 7.5 Results and discussion

### 7.5.1 In-vivo methods of Darunavir loaded solid lipid nanoparticles

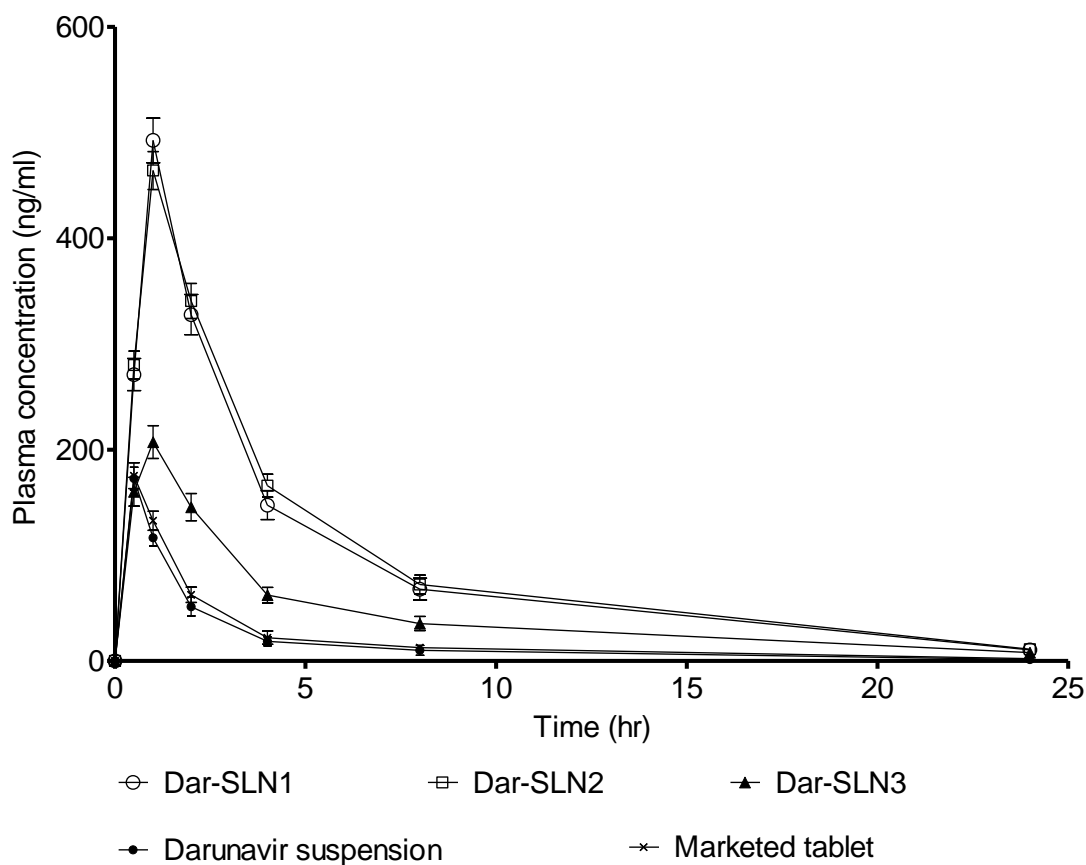
#### 7.5.1.1 Pharmacokinetic profile comparison of three different sized- Darunavir loaded solid lipid nanoparticles

Table 7.1 shows the plasma drug concentration for Darunavir suspension, Darunavir marketed tablet and all three selected Darunavir loaded solid lipid nanoparticles (Dar-SLN1, Dar-SLN2 and Dar-SLN3) at different time points after single oral dose administration in rats (n=3). The plasma concentration of drug versus time profile is depicted in Figure 7.1. The pharmacokinetic parameters including  $C_{max}$ ,  $T_{max}$ ,  $AUC_{0-\infty}$ , plasma half life ( $T_{1/2}$ ) and relative bioavailability were analyzed by Kinetica software 5.0 version and the results obtained are given in Table 7.2.

**Table 7.1 Plasma concentration profile after oral administration of Darunavir suspension, marketed tablet, Dar-SLN1, Dar-SLN2 and Dar-SLN3 to rats (n=3)**

Time (hr)	Darunavir concentration in plasma (ng/ml)				
	Darunavir suspension	Marketed Tablet (DARUVIR)	Dar-SLN1	Dar-SLN2	Dar-SLN3
0	0	0	0	0	0
0.5	172.67 ± 10.67	175.33 ± 12.23	270.99 ± 15.21	280.12 ± 13.12	160.2 ± 13.67
1	116.58 ± 7.56	132.72 ± 9.01	492.66 ± 21.23	464.14 ± 17.89	207.19 ± 15.56
2	51.45 ± 8.82	62.54 ± 7.23	327.84 ± 19.01	340.7 ± 16.64	145.59 ± 12.82
4	18.6 ± 4.27	22.06 ± 6.32	147.5 ± 13.67	165.92 ± 10.87	62.3 ± 7.27
8	10.03 ± 4.65	12.58 ± 4.18	68.02 ± 10.23	72.3 ± 8.98	35.48 ± 6.65
24	1.40 ± 0.60	2.24 ± 0.98	10.57 ± 3.54	11.21 ± 3.12	8.07 ± 4.21

\*Values are represented as mean ± SD, n=3



**Figure 7.1 Comparison of plasma concentration vs time profile after oral administration of Darunavir suspension, marketed tablet, Dar-SLN1, Dar-SLN2 and Dar-SLN3 to rats**

**Table 7.2 Pharmacokinetic parameters after oral administration of Darunavir suspension, marketed tablet, Dar-SLN1, Dar-SLN2 and Dar-SLN3 to rats (n=3)**

Parameter	Darunavir suspension	Marketed Tablet	Dar-SLN1	Dar-SLN2	Dar-SLN3
$C_{max}$ (ng/ml)	172.67±10.67	175.33±12.23	492.66±21.23	464.14±17.89	207.19±15.56
$T_{max}$ (hr)	0.5	0.5	1	1	1
$AUC_{0-t}$ (ng.hr/ml)	418.27±87.86	489.66±91.88	1963.68 ± 213.30	2013.36 ± 285.16	1060.13 ± 159.72
$AUC_{0-∞}$ (ng.hr/ml)	429.27 ± 93.06	508.05 ± 100.85	2039.35 ± 247.52	2097.8 ± 314.52	1144.26 ± 217.00
$T_{1/2}$ (hr)	5.41 ± 0.42	5.89 ± 0.50	5.39 ± 0.52	5.32 ± 0.43	6.83 ± 1.48

MRT (hr)	4.39 ± 0.73	5.00 ± 0.86	6.39 ± 0.64	6.69 ± 0.25	7.37 ± 1.74
Relative bioavailability (%)	-	117.06	469.47	481.35	253.45

\*Values are represented as mean ± SD, n=3

There was a significant increase in  $C_{max}$  ( $P < 0.05$ ) upon nanoparticle administration in comparison to plain drug suspension and marketed tablet. There was 2.85, 2.68 and 1.19 fold increase in  $C_{max}$  of Dar-SLN1, Dar-SLN2 and Dar-SLN3 respectively in comparison to plain drug suspension. Similarly there was significant increase in  $AUC_{0-\infty}$  for SLN formulations ( $P < 0.05$ ) in comparison to plain drug suspension and marketed tablet. The  $AUC_{0-\infty}$  increased by 4.69, 4.81 and 2.53 fold for Dar-SLN1, Dar-SLN2 and Dar-SLN3 respectively relative to plain drug suspension. Since the  $T_{max}$  for SLN formulation was longer along with prolonged release in comparison to plain drug suspension and marketed tablet, one of the possible reason for enhanced bioavailability from SLNs could be the enterocyte formation and absorption of lipids via intestinal lymphatics. SLNs can induce the stimulation of chylomicron formation by enterocytes promoting the lipid absorption through intestinal lymphatics by transcellular route (9).

Among different nanoparticle formulations,  $C_{max}$ , AUC and relative bioavailability of Dar-SLN1 and Dar-SLN2 were significantly higher in comparison to Dar-SLN3 suggesting that nanoparticles of size ~100 nm and ~200 nm gave higher bioavailability than particle of size ~500 nm. The paired t-test suggested a significant difference in  $C_{max}$  of Dar-SLN1 and Dar-SLN2 but a non significant difference in their  $AUC_{0-\infty}$ . The highest relative bioavailability of 481.35 % was found in Dar-SLN2 (~200 nm particles) formulation. Further reduction in particle size to ~100 nm as obtained in Dar-SLN1 led to no significant improvement in bioavailability suggesting that the optimum size of solid lipid nanoparticles for enhancing bioavailability of Darunavir is around 200 nm. A work by Thommes et al. (2) suggested an increase in oral bioavailability of Darunavir using K-carrageenan as pelletisation aid in comparison to marketed tablet likely due to better disintegration and release profile of Darunavir. The

enhancement in bioavailability of Darunavir in our work could be attributed to the enhanced absorption and lymphatic uptake of nanoparticles. This is supported by work done by Alex et al. (9) who revealed SLNs (having mean particle size 230 nm) as lipid vehicle in passive targeting of Lopinavir to intestinal lymphatic region and enhancement in its bioavailability by the use of solid lipid nanoparticles upon oral administration. In addition, it is reported that the use of long chain fatty acids stimulates lipoprotein formation and bypasses the portal circulation through intestinal lymph uptake (10). Hence, Dar-SLN2 was considered as optimized formulation for the purpose of enhancing oral bioavailability of Darunavir.

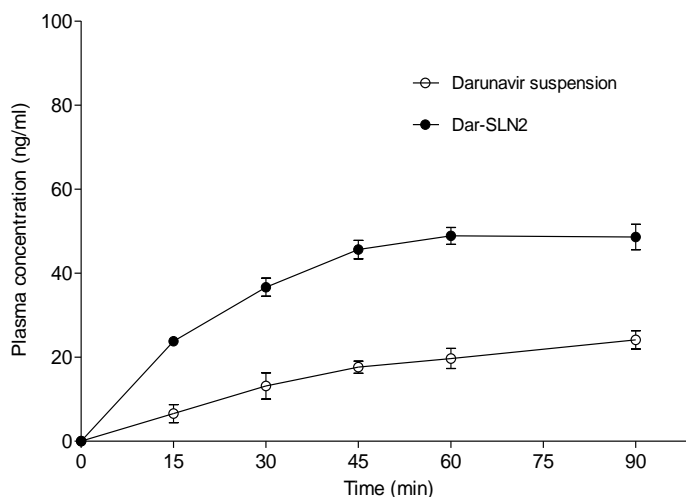
#### **7.5.1.2 *In-situ* absorption from stomach and intestine**

The results of absorption of Darunavir suspension and Darunavir loaded nanoparticles after intragastric administration is shown in Table 7.3 and Figure 7.2. There was significant enhancement in plasma concentration upon administration of nanoparticles (Dar-SLN2) in comparison to free drug suspension.  $AUC_{0-t}$  for Dar-SLN2 increased by 2.50 fold in comparison to  $AUC_{0-t}$  for suspension. The reason for enhanced absorption could be the ability of solid lipid nanoparticles in improving solubilization capacity of drug in the GI tract (11). Similarly, the absorption of Darunavir was also studied upon intraduodenal administration. The results are shown in Table 7.4 and Figure 7.4 depicting enhanced plasma concentrations after nanoparticle administration in comparison to plain drug suspension.  $AUC_{0-t}$  for Dar-SLN2 increased by 2.51 fold in comparison to  $AUC_{0-t}$  for suspension. There was significant enhancement of AUC from Dar-SLN2 as compared to plain drug suspension upon intragastric and intraduodenal administration (Figure 7.3 and Figure 7.5). It could be thereby deduced that the absorption of Darunavir from the GI tract could be greatly improved after incorporation into SLNs. In addition, the AUC of Dar-SLN2 after intragastric administration was only 11.8 % of the AUC after intraduodenal administration, which indicated that the absorption of SLNs mainly occurred in the intestine.

**Table 7.3 Mean plasma Darunavir concentration after intragastric administration of Darunavir suspension and optimized Darunavir loaded SLNs (Dar-SLN2)**

Time (min)	Mean plasma concentration of Darunavir from drug suspension (ng/ml) $\pm$ SD	Mean plasma concentration of Darunavir from Dar-SLN2 (ng/ml) $\pm$ SD
0	0	0
15	6.57 $\pm$ 2.13	23.78 $\pm$ 1.02
30	13.15 $\pm$ 3.12	36.67 $\pm$ 2.13
45	17.63 $\pm$ 1.43	45.61 $\pm$ 2.2
60	19.7 $\pm$ 2.38	48.87 $\pm$ 2.0
90	24.12 $\pm$ 2.17	48.60 $\pm$ 3.03
AUC <sub>0-t</sub> (ng.hr/ml)	22.75 $\pm$ 3.10	56.98 $\pm$ 2.89

\*n=3

**Figure 7.2 Plasma concentration of Darunavir from Darunavir suspension and Dar-SLN2 after intragastric administration**

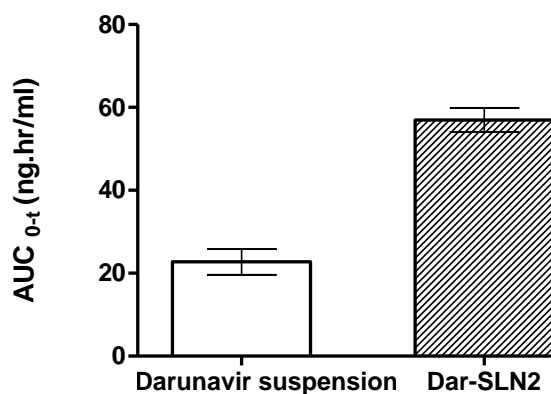


**Figure 7.3 Comparison of AUC<sub>0-t</sub> obtained after intragastric administration of Darunavir suspension and optimized Darunavir loaded SLNs (Dar-SLN2)**

**Table 7.4 Mean plasma Darunavir concentration after intraduodenal administration of Darunavir suspension and optimized Darunavir loaded SLNs (Dar-SLN2)**

Time (min)	Mean plasma concentration of Darunavir from plain drug suspension (ng/ml)	Mean plasma concentration of Darunavir from Dar-SLN2 (ng/ml)
0	0	0
15	123.22 ± 7.18	145.1 ± 10.62
30	189.45 ± 11.31	286.63 ± 17.71
45	157.43 ± 10.45	390.45 ± 17.43
60	132.29 ± 10.47	484.38 ± 23.35
90	95.15 ± 2.62	368.69 ± 15.41
AUC <sub>0-t</sub> (ng.hr/ml)	190.92 ± 11.81	479.35 ± 24.04

\*Values are represented as mean  $\pm$  SD, n=3

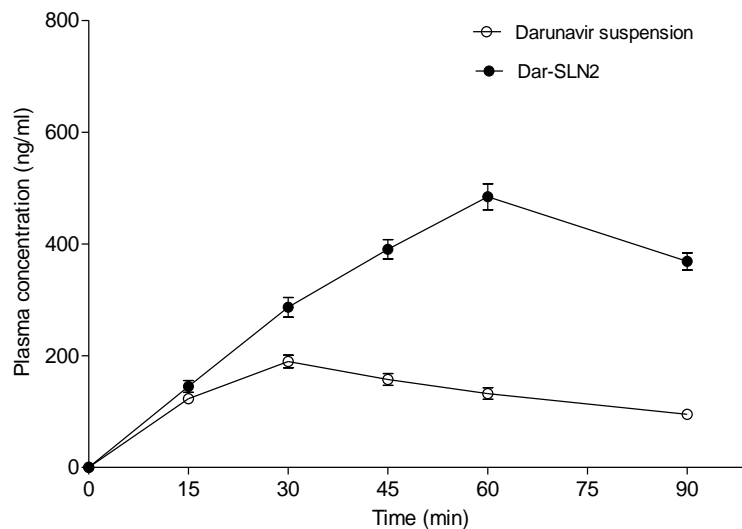


**Figure 7.4 Plasma concentration of Darunavir from Darunavir suspension and Dar-SLN2 after intraduodenal administration**

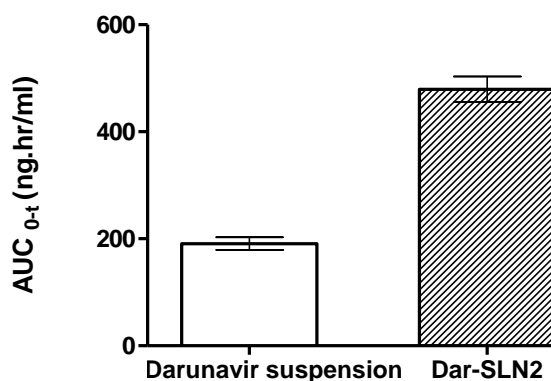


**Figure 7.5 Comparison of AUC<sub>0-t</sub> obtained after intraduodenal administration of Darunavir suspension and optimized Darunavir loaded SLNs (Dar-SLN2)**

### 7.5.1.3 Lymphatic transport study

To investigate the subsequent transport of SLNs after its uptake into the enterocytes, cycloheximide was used to inhibit the lymphatic transport pathway without nonspecific damage to other active and passive absorption pathways. As seen from the results (Table 7.5 and Figure 7.6), the plasma concentration of Darunavir in rats treated with cycloheximide was lower than that treated with saline at all time periods. When Dar-

SLN2 was intraduodenally administered to rats pre-treated with cycloheximide, the peak concentration ( $C_{max}$ ) of Darunavir was significantly reduced by 55.78% ( $P < 0.05$ ) and the  $AUC_{0-t}$  value (Figure 7.7) decreased by 59.15% ( $P < 0.05$ ), which could be attributed to the blockage of intestinal lymphatic transport by cycloheximide. Therefore, it could be speculated that the lymphatic transport pathway played an important role in the intestinal transport of SLNs into the systemic circulation (11).

**Table 7.5 Plasma concentration of Darunavir from Dar-SLN2 in presence and absence of cycloheximide**

<b>Time (min)</b>	<b>Mean plasma concentration Darunavir from Dar-SLN2 along with saline (ng/ml)</b>	<b>Mean plasma concentration of Darunavir from Dar-SLN2 along with cycloheximide (ng/ml)</b>
0	0	0
15	143.1 ± 8.51	64.83 ± 10.72
30	289.63 ± 15.12	148.18 ± 18.65
45	392.45 ± 17.19	225.88 ± 17.51
60	479.38 ± 22.95	290.52 ± 22.23
90	375.69 ± 15.65	242.19 ± 14.23
120	318.2 ± 11.75	187.22 ± 10.1
$C_{max}$	479.38 ± 22.95	290.52 ± 22.23
$AUC_{0-t}$ (ng.hr/ml)	653.45 ± 29.57	386.56 ± 29.69

\*Values are represented as mean ± SD, n=3

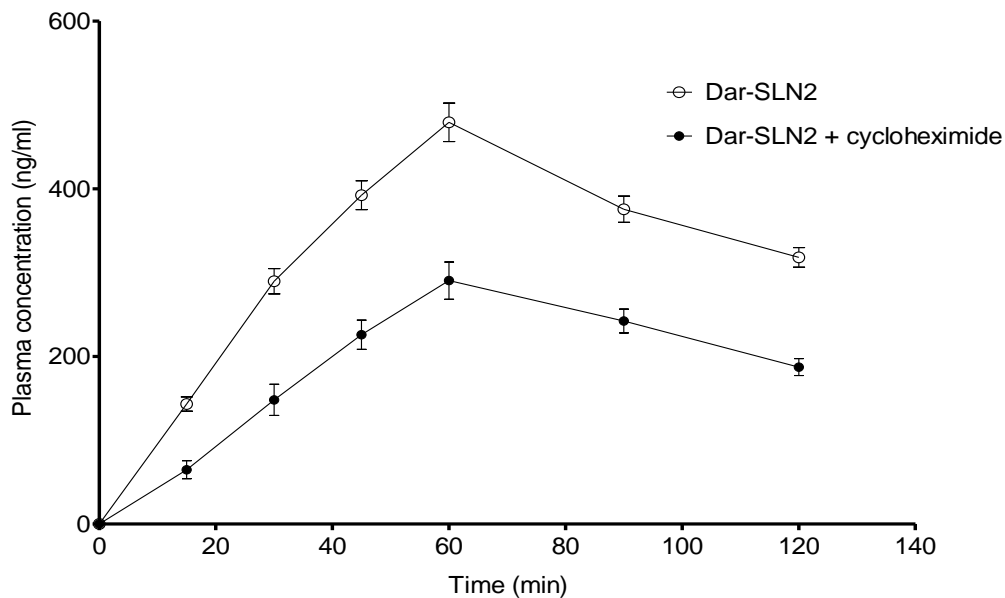


**Figure 7.6 Plasma concentration versus time profile of Darunavir from Dar-SLN2 in presence and absence of cycloheximide**

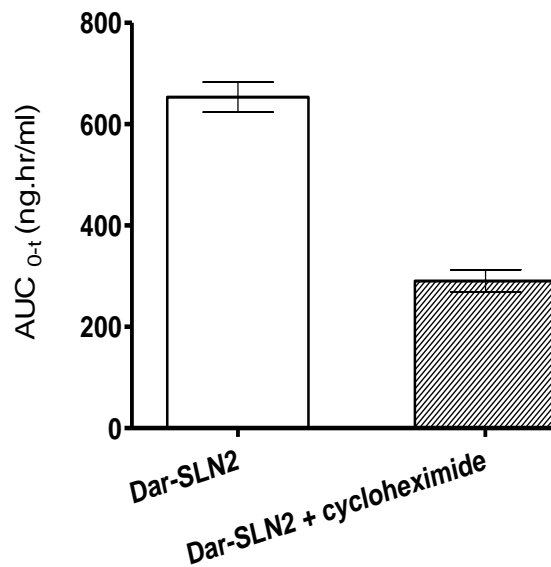


**Figure 7.7 Comparison of AUC<sub>0-t</sub> of Darunavir upon Dar-SLN2 administration in presence and absence of cycloheximide**

#### 7.5.1.4 Organ biodistribution study

Biodistribution pattern of Darunavir in different organs upon plain drug suspension and SLN (Dar-SLN2) administration was studied and the results are shown in Table 7.6

and Table 7.7. The comparison of drug concentration for plain drug suspension and Dar-SLN2 in each organ is depicted in Figure 7.8 and Figure 7.9.

**Table 7.6 Results of biodistribution study in different organs upon administration of Darunavir suspension**

Time (hr)	Darunavir concentration ( $\mu\text{g/g}$ of organ) in various organs upon administration of Darunavir suspension							
	Liver	Spleen	Kidney	Heart	Lung	Stomach	Intestine	Brain
1	282.57 $\pm 13.1$ 2	124.75 $\pm 11.16$	165.56 $\pm 13.32$	16.62 $\pm 3.11$	20.08 $\pm 3.02$	377.42 $\pm 16.23$	476.84 $\pm 26.3$	61.22 $\pm 10.34$
4	328.3 $\pm 15.2$ 3	55.27 $\pm 9.9$	108.52 $\pm 10.43$	13.48 $\pm 3.21$	18.07 $\pm 3.37$	235.7 $\pm 13.71$	245.56 $\pm 11.28$	32.37 $\pm 8.32$
8	203.71 $\pm 10.7$ 2	38.68 $\pm 8.32$	80.93 $\pm 9.54$	8.98 $\pm 2.63$	12.05 $\pm 3.9$	150.54 $\pm 10.04$	110.21 $\pm 8.23$	25.18 $\pm 6.34$
24	115.74 $\pm 8.31$	11.05 $\pm 6.32$	23.38 $\pm 5.32$	2.24 $\pm 0.43$	4.02 $\pm 2.13$	75.45 $\pm 9.9$	65.82 $\pm 7.33$	21.25 $\pm 3.43$

\*Values are represented as mean  $\pm$  SD, n=3

**Table 7.7 Results of biodistribution study in different organs upon administration of Darunavir loaded SLNs**

Time (hr)	Darunavir concentration ( $\mu\text{g/g}$ of organ) in various organs upon administration of Darunavir loaded SLNs (Dar-SLN2)							
	Liver	Spleen	Kidney	Heart	Lung	Stomach	Intestine	Brain
1	184 $\pm 6.32$	221.08 $\pm 12.35$	56.22 $\pm 8.28$	40.44 $\pm 3.23$	36.15 $\pm 2.84$	657.44 $\pm 25.23$	392.6 $\pm 14.43$	93.28 $\pm 9.23$
4	197.14 $\pm 10.2$ 1	165.81 $\pm 10.31$	113.53 $\pm 10.01$	31.45 $\pm 2.1$	24.1 $\pm 2.75$	352.7 $\pm 15.56$	523.21 $\pm 22.49$	115.34 $\pm 11.45$
8	131.42 $\pm 5.12$	142.45 $\pm 9.4$	151.37 $\pm 17.97$	17.97 $\pm 2.23$	20.56 $\pm 2.43$	211.61 $\pm 13.42$	280.19 $\pm 13.27$	76.2 $\pm 9.7$
24	85.97 $\pm 3.22$	88.29 $\pm 7.13$	47.29 $\pm 7.43$	0.85 $\pm 0.15$	12.04 $\pm 2.32$	76.58 $\pm 11.23$	191.45 $\pm 12.28$	54.35 $\pm 6.34$

\*Values are represented as mean  $\pm$ SD, n=3

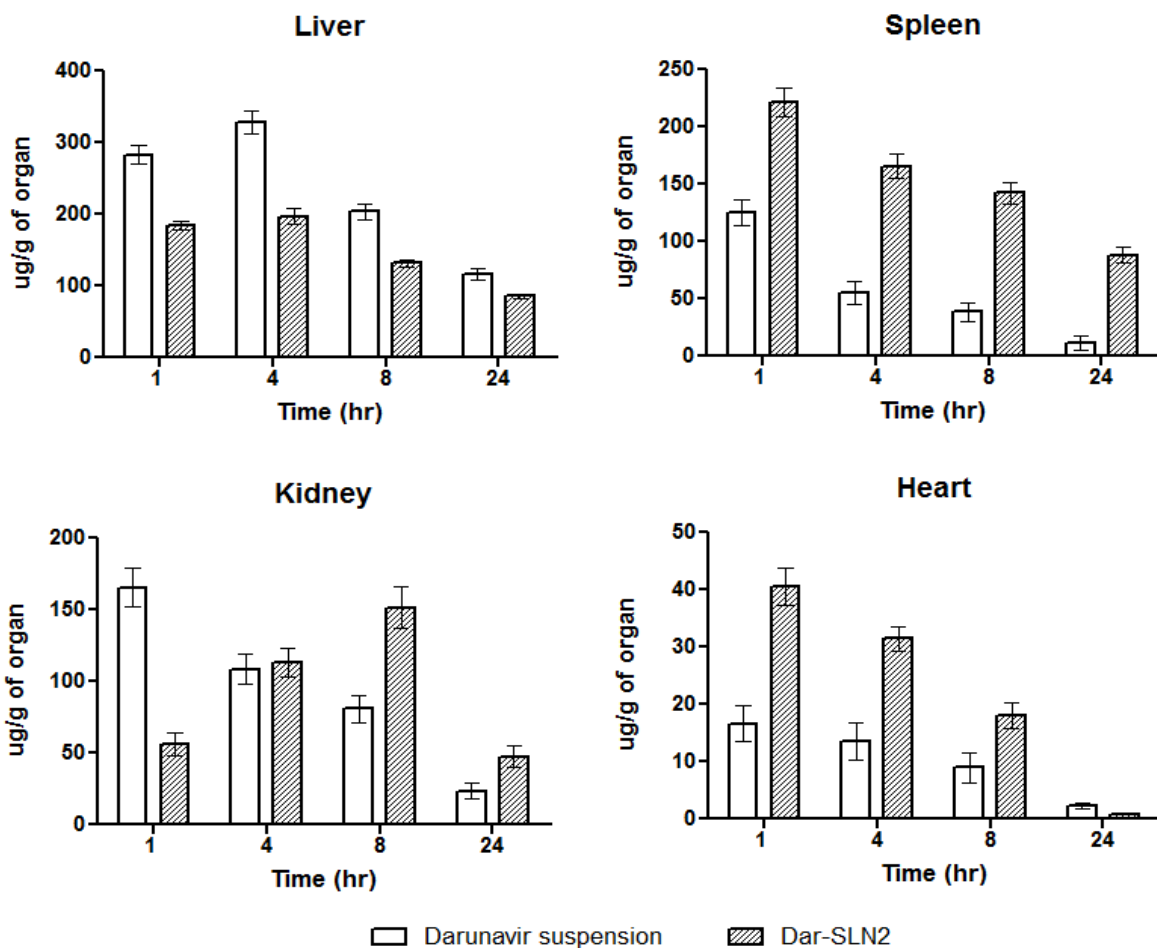


**Figure 7.8 Comparison of Darunavir concentration obtained in liver, spleen, kidney, and heart upon administration of plain drug suspension and Darunavir loaded SLNs**

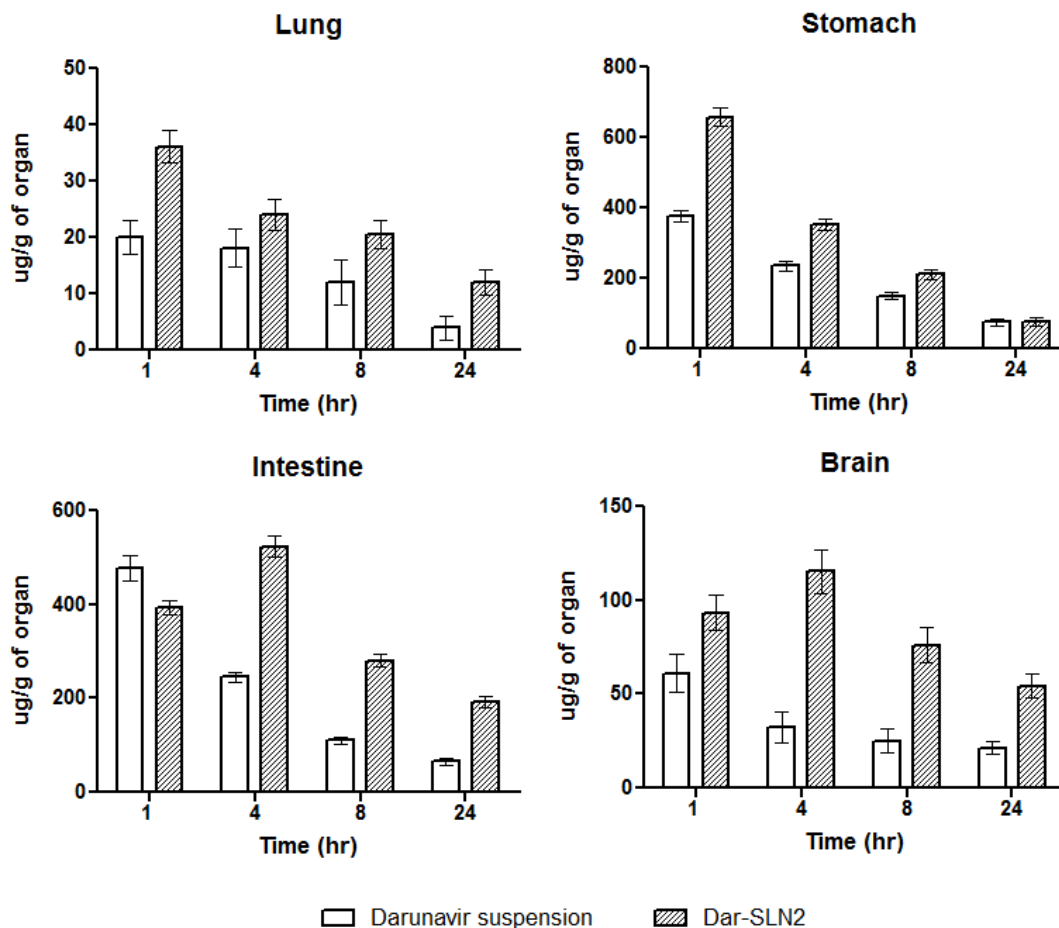


**Figure 7.9 Comparison of Darunavir concentration obtained in lung, stomach, intestine and brain upon administration of plain drug suspension and Darunavir loaded SLNs**

Dar-SLN2 showed a higher distribution of Darunavir than from plain drug suspension form as demonstrated by an increased impregnation of virtually all investigated tissues except liver. The order of Darunavir AUC from highest to lowest for Dar-SLN2 formulation was as follows: intestine > stomach > spleen > Liver > kidney > brain > lung > heart. An initial higher uptake was found in the intestine (due to rapid uptake by GI tract upon administration) followed by a subsequent decrease indicating distribution into other organs. The clearance of Darunavir from nanoparticles was slower than that given in suspension as indicated by a gradual increase in concentrations in kidney up to 8 hr while in suspension form, it showed clearance in the first hr. Major HIV reservoir organs namely, spleen and brain showing higher Darunavir concentration upon

nanoparticle administration indicate the superiority of nanoparticulate systems in increasing the accumulation of drug in various target organs. The transport of most protease inhibitors including Darunavir across the blood-brain barrier is reported to be very poor (12). Figure 7.9 compares the brain concentration of Darunavir after its administration in form of drug suspension and nanoparticles. The results showed a 1.5-3.5 fold higher accumulation of Darunavir in brain when administrated through solid lipid nanoparticles compared to suspension. This was due to the inherent ability of nanoparticles to cross the BBB by opening the tight junction between endothelial cells (13). This would lead to increased retention of nanoparticles in the brain capillaries combined with absorption through capillary walls by receptor mediated endocytosis (14, 15). Since Darunavir is extensively metabolized in liver, its lower concentration in liver upon Dar-SLN2 administration is of great therapeutic benefit. Moreover, kidney showed decreased drug concentration in initially hours in nanoparticle formulation indicating a delayed clearance of drug from the body. This data is supported by the pharmacokinetic study where mean residence time was found to be higher in nanoparticle formulation (6.69 hr) compared to plain drug suspension (4.39 hr).

#### **7.5.1.5 Biodistribution of SLNs in Peyer's patch (PP) and Non-peyer's (Non-PP) patch**

Figure 7.10 shows the intestine section cut open before treatment with acetic acid. Peyer's patch region can be seen as round dark region as compared to other section. The same section were then stained using acetic acid to fix the nuclei. After treatment with acetic acid, the same region was seen as raised white areas as seen in Figure 7.11. Because the peyer's patches consist almost entirely of nuclear material, the fixed patches stand out clearly as white opaque superficial plaques (16).

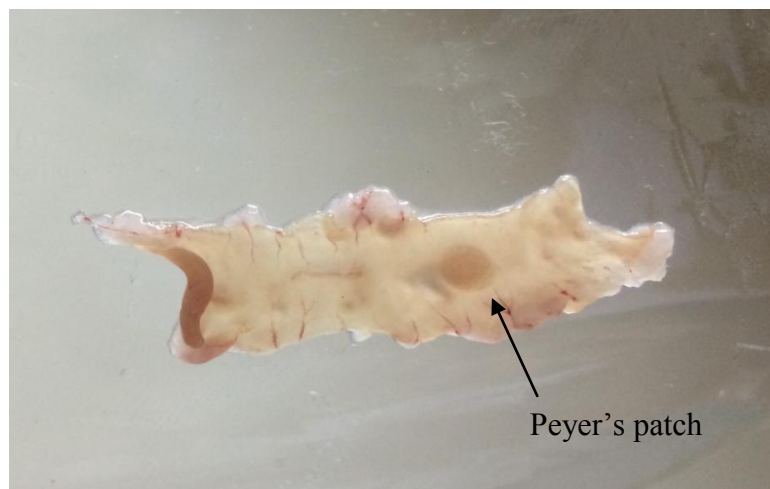


**Figure 7.10 Photographic image of section of intestine before treatment with acetic acid**

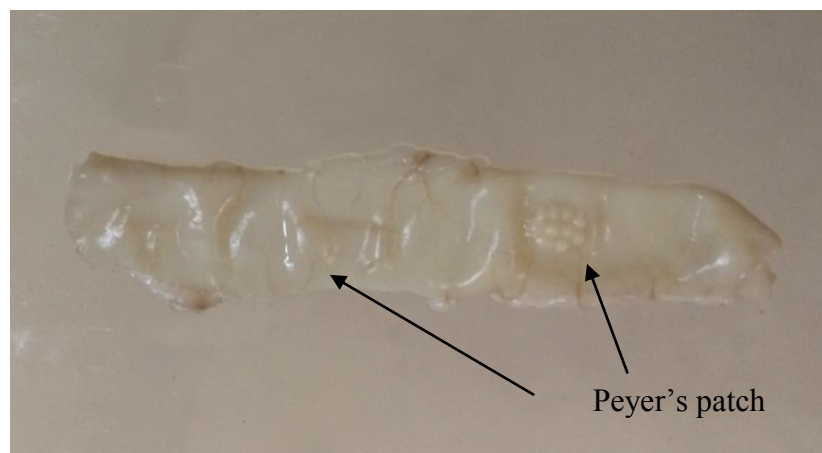


**Figure 7.11 Photographic image of section of intestine after treatment with acetic acid**

Dar-SLN2 was administered to rats orally, the PP and non-PP regions were separated and the amount of Darunavir in them was quantified by LCMS. The results are shown Table 7.8 and Figure 7.12. There was significant difference between the drug concentrations in both the regions ( $P < 0.05$ ). It was observed that the Darunavir amount in PP region was 4.12 fold higher as compared to non-PP region. A higher concentration in PP region observed is due to the size of nanoparticles. In other studies, investigators have used particles of micron size range and demonstrated that PLGA particles  $> 5 \mu\text{m}$  in diameter cannot traverse in the peyer's patch and are not seen systemically (17). Similar studies (other than nanoparticles) by Ebel (18) showed greater uptake of  $< 5 \mu\text{m}$

fluorescent polystyrene latex particles in the Peyer's patch in mice. In addition, study done using 100nm, 500 nm, 1  $\mu$ m and 10  $\mu$ m polymeric nanoparticles demonstrated that particles of size 100 nm were taken by PP region more in comparison to other particles (5). It is also hypothesized by Florence et al. (19) that nanoparticles because of their smaller size would also have an efficient disposition via Peyer's patch to other lymphatic organs such as to the mesenteric lymph nodes and to spleen.

**Table 7.8 Distribution of Darunavir in PP and Non-PP region upon oral administration of Dar-SLNs**

Time (hr)	Amount of Darunavir ( $\mu$ g/mg of tissue)	
	Peyer's patch	Non-peyer's patch
1	0.84 $\pm$ 0.23	0.25 $\pm$ 0.04
4	1.3 $\pm$ 0.35	0.32 $\pm$ 0.19
8	0.65 $\pm$ 0.31	0.12 $\pm$ 0.08
24	0.43 $\pm$ 0.11	0.09 $\pm$ 0.03

\*Values are represented as mean  $\pm$  SD, n=3

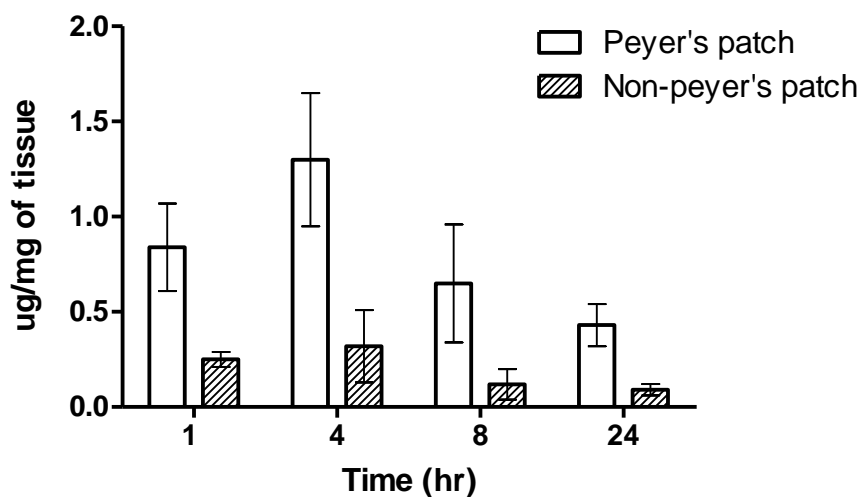


**Figure 7.12 Comparison of Darunavir amount in PP and Non-PP region upon oral administration of Dar-SLNs**

## 7.5.2 In-vivo methods of optimized Peptide-grafted Darunavir loaded SLNs (Pept-Dar-SLN)

### 7.5.2.1 Pharmacokinetic study

The results of pharmacokinetics of peptide grafted SLNs loaded with Darunavir is given in Table 7.9. The comparison of plasma concentration versus time profile for peptide grafted and non-peptide grafted SLNs loaded with Darunavir is shown in Figure 7.13. Pharmacokinetic parameters are given in Table 7.10 along with its comparison to non-peptide grafted SLNs (Dar-SLN2). The experimental results indicated that the plasma concentration of Darunavir in rats after oral administration of SLNs and peptide grafted SLNs showed no significant difference ( $P>0.5$ ). It indicated that the grafting of peptide had no effect on its pharmacokinetic profile.

**Table 7.9 Plasma concentration vs time profile after oral administration of peptide grafted Darunavir SLNs (Pept-Dar-SLN) and non-peptide grafted Darunavir SLNs (Dar-SLN2) to rats (n=3)**

Time (hr)	Darunavir concentration in plasma (ng/ml)
0	0
0.5	261.45 ± 10.11
1	452.31 ± 16.23
2	332.56 ± 11.32
4	181.23 ± 9.34
8	80.23 ± 10.23
24	8.17 ± 4.18

\*Values are represented as mean ± SD, n=3

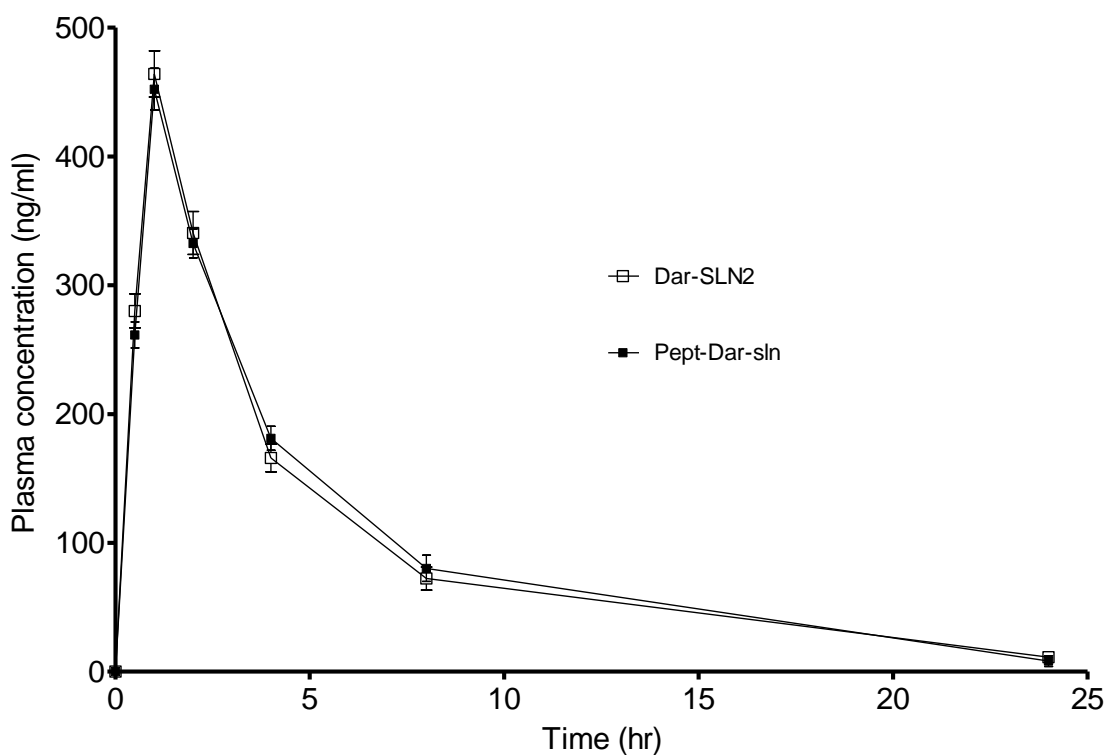


**Figure 7.13** Comparison of plasma concentration vs time profile after oral administration of peptide grafted Darunavir SLNs (Pept-Dar-SLN) and non-peptide grafted Darunavir SLNs (Dar-SLN2) rats (n=3)

**Table 7.10** Pharmacokinetic parameters after oral administration of peptide grafted Darunavirs SLNs (Pept-Dar-SLN) and non-peptide grafted Darunavir SLNs (Dar-SLN2) rats (n=3)

Parameter	Pept-Dar-SLN	Dar-SLN2
C <sub>max</sub> (ng/ml)	452.31 ± 16.23	464.14 ± 17.89
T <sub>max</sub> (hr)	1	1
AUC <sub>0-t</sub> (ng.hr/ml)	2380.14 ± 197.96	2013.36 ± 285.16
AUC <sub>0-∞</sub> (ng.hr/ml)	2434.92 ± 232.65	2097.8 ± 314.52
T <sub>1/2</sub> (hr)	4.5 ± 0.73	5.32 ± 0.43
MRT	5.39 ± 0.67	6.69 ± 0.25

### 7.5.2.2 Organ biodistribution study

Biodistribution of Darunavir upon administration of peptide grafted nanoparticles was studied and the results are shown in Table 7.11. The comparison of drug concentrations in various organs for peptide grafted and non-peptide grafted SLNs is depicted in Figure 7.14 and Figure 7.15. The order of Darunavir AUC in various organs from highest to lowest for Pept-Dar-SLN is as follows: intestine > stomach > spleen > liver > kidney > brain > heart > lung. There was significant difference found between the drug concentrations in spleen and liver for peptide grafted and non-peptide grafted nanoparticles which is likely due to the presence of peptide on nanoparticle surface leading to higher binding with T-cells present in liver and spleen. In other organs, no statistical differences were observed between distributions of both the nanoparticles.

**Table 7.11 Results of biodistribution study in different organs upon administration of peptide grafted Darunavir loaded SLNs**

Time (hr)	Darunavir concentration ( $\mu\text{g/g}$ of organ) in various organs upon administration of Pept-Dar-SLN							
	Liver	Spleen	Kidney	Heart	Lung	Stomach	Intestine	Brain
1	161.1 $\pm 7.89$	288.9 $\pm 15.67$	60.23 $\pm 10.2$	39.54 $\pm 5.45$	40.11 $\pm 3.23$	630.12 $\pm 36.45$	371.67 $\pm 13.23$	95.4 $\pm 10.1$
4	183.1 2 $\pm 12.4$ 5	212.00 $\pm 21.32$	105.31 $\pm 13.23$	35.87 $\pm 6.34$	27.34 $\pm 3.45$	382.23 $\pm 25.34$	500.14 $\pm 24.86$	110.3 $\pm 10.23$
8	110.1 1 $\pm 8.99$	167.1 $\pm 10.73$	137.89 $\pm 10.67$	20.32 $\pm 3.23$	18.55 $\pm 3.1$	189.34 $\pm 17.28$	260.21 $\pm 15.67$	82.32 $\pm 7.86$
24	64.23 $\pm 9.92$	94.56 $\pm 9.9$	40.85 $\pm 6.34$	1.12 $\pm 0.4$	10.23 $\pm 4.23$	65.82 $\pm 12.32$	171.23 $\pm 16.34$	64.2 $\pm 10.26$

\*Values are represented as mean  $\pm$  SD, n=3

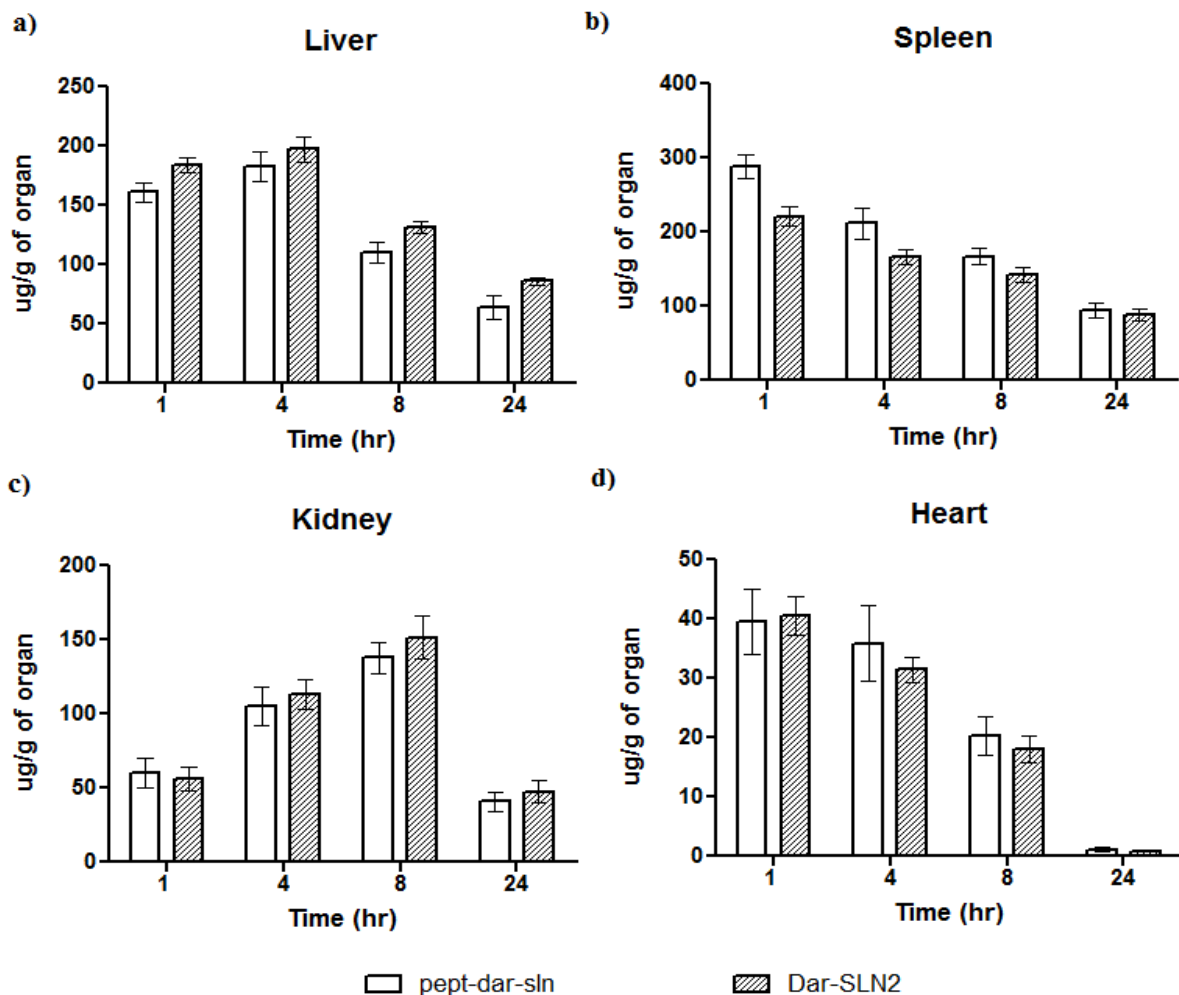


**Figure 7.14 Comparison of Darunavir concentration obtained in liver, spleen, kidney, and heart upon administration of peptide grafted- and non-peptide grafted SLNs of Darunavir**

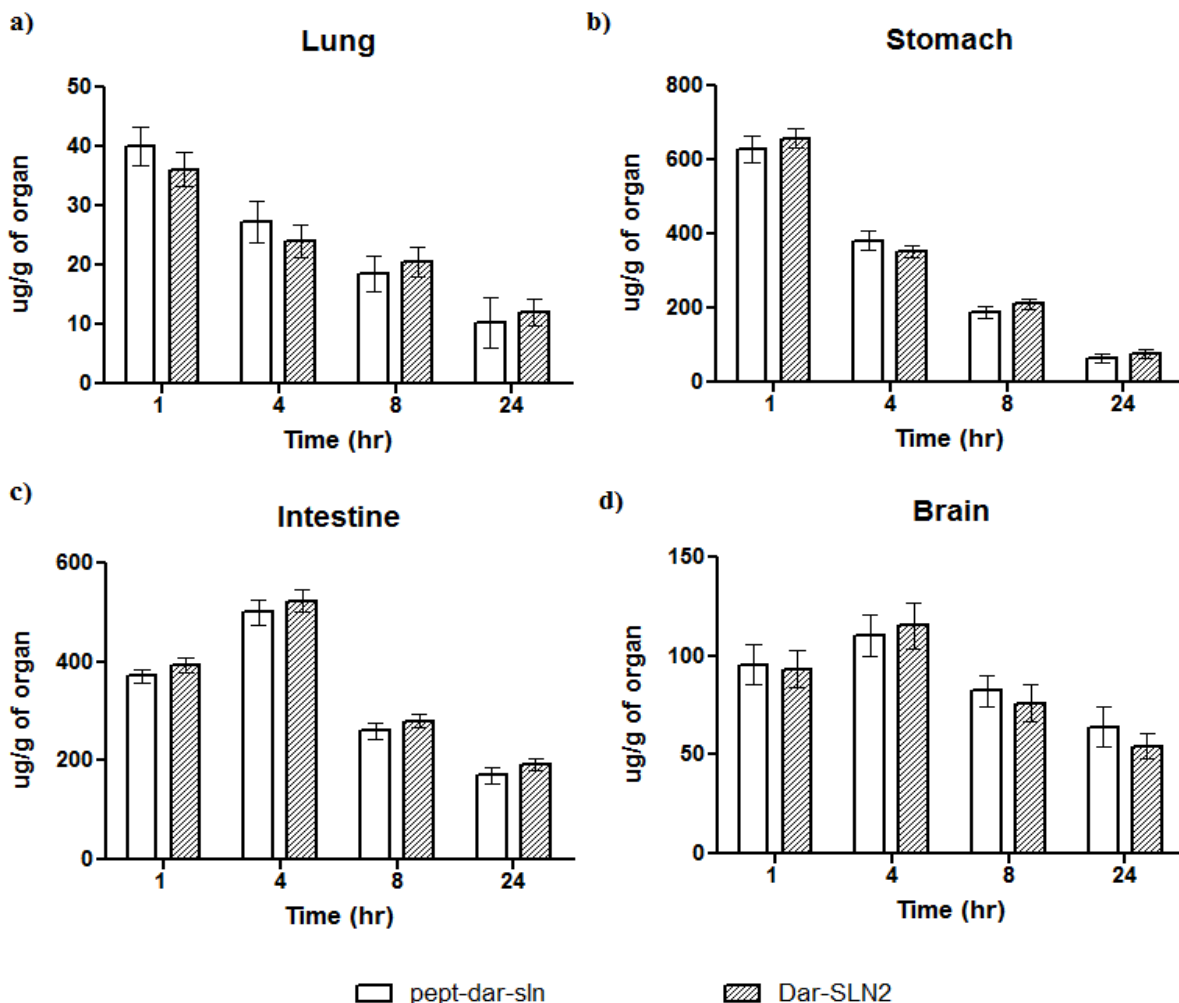


**Figure 7.15 Comparison of Darunavir concentrations obtained in lung, stomach, intestine and brain upon administration of peptide grafted- and non-peptide grafted SLNs of Darunavir**

### 7.5.3 In-vivo methods of optimized Darunavir loaded Nanoemulsion (DNE-3)

#### 7.5.3.1 Pharmacokinetic study

Table 7.12 shows the plasma drug concentration for Darunavir lipid nanoemulsion along with its comparison with Darunavir suspension and marketed tablet after oral administration in rats ( $n=3$ ). Their plasma Darunavir concentration versus time profile is depicted in Figure 7.16. The non-compartmental kinetics parameters were calculated (Figure 7.16 and Table 7.13) to evaluate the absorption behavior of Darunavir lipid

nanoemulsion (DNE-3). In comparison to pure Darunavir and marketed tablet, DNE-3 showed significantly higher plasma drug profiles. The peak drug concentration ( $C_{max}$ ) of DNE-3 ( $231.89 \pm 13.22$  ng/ml) was approximately 1.99 fold higher than suspension form ( $116.58 \pm 7.56$  ng/ml). The high solubility of Darunavir in the oil phase leads to slower release into the outer aqueous phase that is reflected in the higher ( $T_{max}$ ) observed for lipid nanoemulsion (1hr). Similarly, other parameters like biological half life, mean residence time and area under curve were found to be significantly higher in comparison to both, Darunavir suspension and marketed tablet.

**Table 7.12 Plasma concentration profile after oral administration of Darunavir nanoemulsion in comparison to its suspension form and Marketed tablet (n=3)**

Time (hr)	Darunavir concentration in plasma (ng/ml)		
	DNE-3	Darunavir suspension	Marketed tablet
0	0	0	0
0.5	$173.27 \pm 12.83$	$172.67 \pm 10.67$	$175.33 \pm 12.23$
1	$231.89 \pm 13.22$	$116.58 \pm 7.56$	$132.72 \pm 9.01$
2	$139.86 \pm 10.32$	$51.45 \pm 8.82$	$62.54 \pm 7.23$
4	$49.28 \pm 6.83$	$18.6 \pm 4.27$	$22.06 \pm 6.32$
8	$26.78 \pm 5.38$	$10.03 \pm 4.65$	$12.58 \pm 4.18$
24	$6.23 \pm 3.21$	$1.40 \pm 0.60$	$2.24 \pm 0.98$

\*Values are represented as mean  $\pm$  SD, n=3

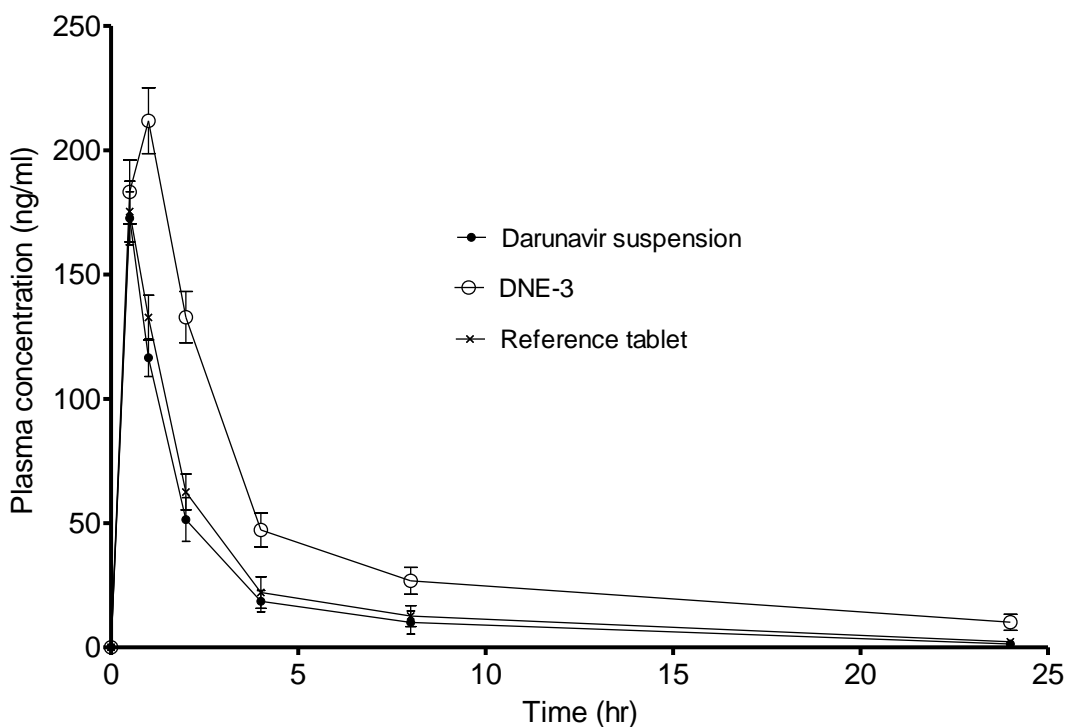


**Figure 7.16 Comparison of plasma concentration versus time profile after oral administration of Darunavir lipid nanoemulsion, Darunavir suspension and marketed tablet**

**Table 7.13 Pharmacokinetic parameters after oral administration of Darunavir nanoemulsion in comparison to its suspension form and marketed tablet (n=3)**

Parameter	Darunavir nanoemulsion	Darunavir suspension	Marketed Tablet (DARUVIR)
$C_{\max}$ (ng/ml)	231.89 ± 13.22	172.67±10.67	175.33±12.23
$T_{\max}$ (hr)	1	0.5	0.5
$AUC_{0-t}$ (ng.hr/ml)	935.82 ± 186.36	418.27±87.86	489.66±91.88
$AUC_{0-\infty}$ (ng.hr/ml)	999.68 ± 174.21	429.27 ± 93.06	508.05 ± 100.85
$T_{1/2}$ (hr)	6.79 ± 1.38	5.41 ± 0.42	5.89 ± 0.50
MRT	6.59 ± 1.58	4.39 ± 0.73	5.00 ± 0.86
Relative	223.76	-	117.06

bioavailability			
-----------------	--	--	--

\*Values are represented as mean  $\pm$  SD, n=3

The bioavailability upon lipid nanoemulsion administration was enhanced by 223 % relative to suspension form. Improvement in bioavailability of Darunavir from DNE-3 can be attributed to many factors which, either in combination or alone contribute for favored magnitude of absorption like lipophilic drug in solution or in small emulsion globules eliminates the dissolution step and keeps drug in a dissolved state during transport to the unstirred water layer of the GI membrane, lymphatic transport through intestinal transcellular pathways. In addition, the vehicles used in formulation (Tween 80) modulate the P-gp efflux pumps (20) and/or CYP450 enzymes function (21) at intestinal region and improve the absorption of drug. Earlier reports suggest that the majority of lipid based systems comprising of long chain/ medium chain fatty acids gain admittance to intestinal lymph and bypass portal circulation, whereas a larger portion of shorter chain lipids get absorbed into the systemic circulation (22). Our results also envisage favoured absorption of Darunavir from DNE-3 formulation because of long chain triglyceride in soyabean oil that enhances lipoprotein synthesis and subsequent lymphatic absorption (23, 24).

### 7.5.3.2 Organ biodistribution study

Biodistribution pattern of Darunavir to different organs upon lipid nanoemulsion administration was studied and the results are shown in Table 7.14. The comparison of its distribution with the suspension form into various organs is depicted in Figure 7.17 and Figure 7.18.

**Table 7.14 Results of biodistribution study in different organs upon administration of Darunavir loaded lipid nanoemulsion**

Time (hr)	Darunavir concentration ( $\mu\text{g/g}$ of organ) in various organs upon administration of DNE-3							
	Liver	Spleen	Kidney	Heart	Lung	Stomach	Intestine	Brain
1	246.26	181.27 $\pm$ 10.23	104.25 $\pm$ 10.10	25.33 $\pm$ 4.12	25.35 $\pm$ 3.19	546.25 $\pm$ 31.23	311.77 $\pm$ 16.67	105.67

	±8.79							±8.1
4	275.2 ±13.2 8	115.63 ±13.25	111.62 ±12.34	17.25 ±4.33	20.32 ±4.23	328.32 ±19.9	351.2 ±26.78	121.32 ±9.9
8	175.3 7 ±6.22	82.58 ±8.24	123.64 ±16.2	10.23 ±2.10	15.27 ±2.75	171.12 ±11.3	188.28 ±16.24	84.9 ±8.24
24	104.2 5 ±4.27	40.75 ±8.12	29.33 ±6.15	0.42 ±0.50	7.25 ±2.11	65.24 ±9.29	119.34 ±14.90	60.22 ±4.28

\*Values are represented as mean ± SD, n=3

There was significant improvement in tissue accumulation of Darunavir into different organs upon lipid nanoemulsion administration in comparison to plain drug suspension. The order of Darunavir AUC from highest to lowest for DNE-3 is as follows: stomach > intestine > liver > spleen > kidney > brain > lung > heart. Upon administration of lipid nanoemulsion, drug remains in solubilized form in the lipidic phase. Hence, higher drug concentrations were found in stomach in initial 1<sup>st</sup> hr in comparison to plain drug suspension. Intestine showed highest absorption at its 4<sup>th</sup> hr which might be due to the slow release of Darunavir from the lipid phase due to its higher solubility in this phase. However, the nanosized droplets give the advantage of higher surface area that increases the rate of drug diffusion into the outer phase of GI fluid. Brain uptake of Darunavir for DNE-3 was observed to be 2.65 fold higher than that for suspension and even 1.09 fold higher than that for Darunavir SLNs (Dar-SLN2). Higher brain uptake of lipid nanoemulsion compared to solid lipid nanoparticles has also been reported earlier (25). SLNs and DNEs differ only in their physical state; SLNs possess solid lipid and DNE contain liquid lipid. However, brain uptake of DNEs was higher possibly due to the advantage of superior flexibility allowing them to squeeze through the endothelial lining. Just like SLNs, DNEs can enter the brain by absorption of DNE globules onto brain capillary walls leading to increased retention of DNE globules in brain capillaries and creating a higher concentration gradient across endothelial cells (26). Endocytosis and transcytosis may also be possible mechanisms for entry of DNEs into brain because of their lipophilic nature. In addition, DNEs contained tween 80 which is known to increase

permeability through BBB. Kreuter (27) has proposed the mechanism for entry of tween 80 containing nanoparticles into brain. The reason for the increased uptake of DNEs containing tween80 across the BBB is most likely due to endocytosis via the LDL receptor by endothelial cells lining brain capillaries. This endocytosis is mediated by the adsorption of Apo-B and/ or Apo-E onto globules from the blood. The DNEs can then mimic the lipoprotein and the drug may either be released within these endothelial cells followed by passive diffusion into the brain or be transported into the brain by transcytosis. Furthermore, tween 80 has the ability to inhibit intestinal P-gp and has been used to increase the permeability of numerous drugs (14) in models of the intestinal wall. Inhibition of P-gp at the BBB may be another mechanism by which tween 80 containing DNEs improve brain levels of Darunavir.

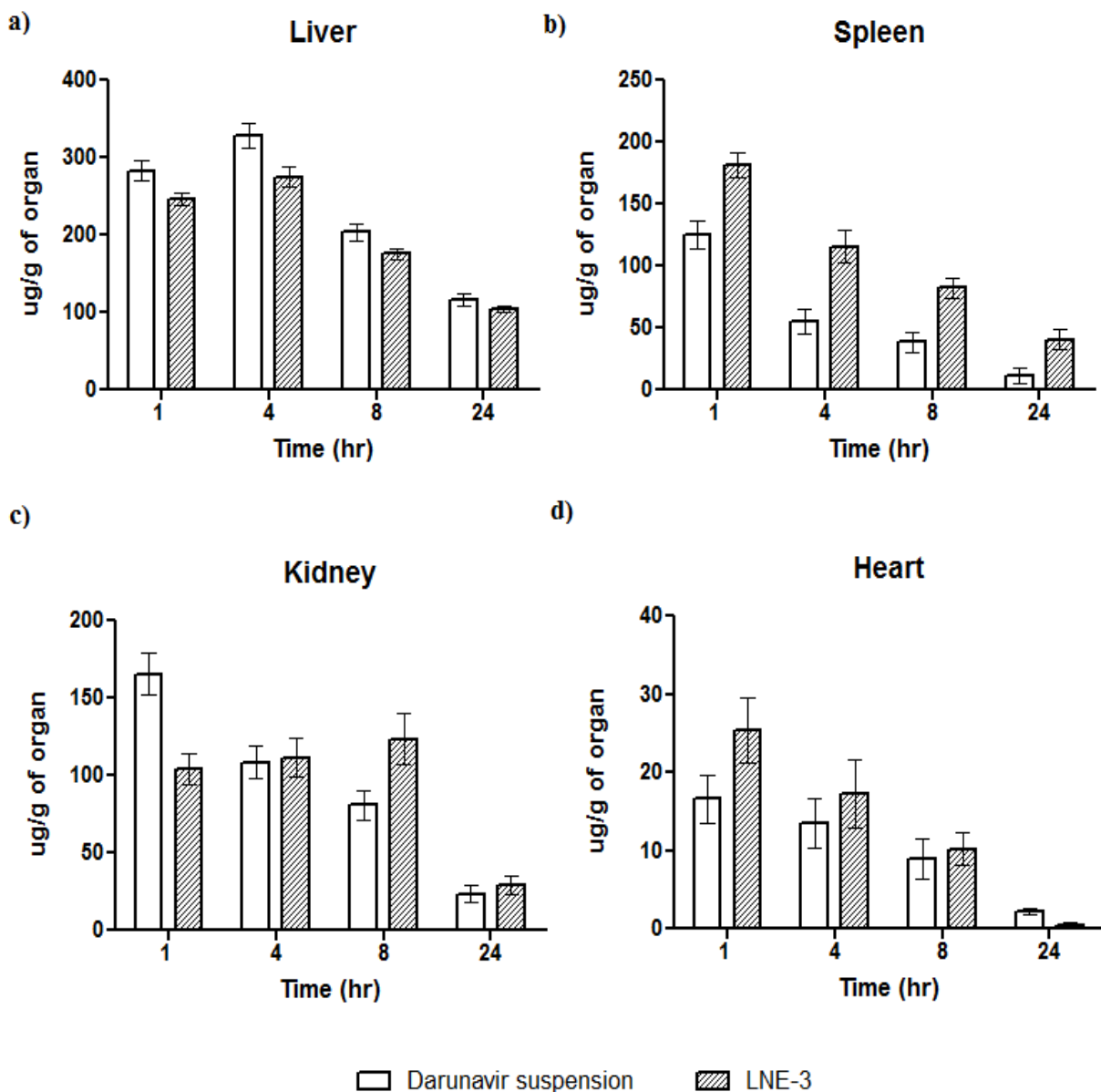


**Figure 7.17 Comparison of Darunavir concentration obtained in liver, spleen, kidney, and heart upon administration of plain drug suspension and Darunavir loaded lipid nanoemulsion**

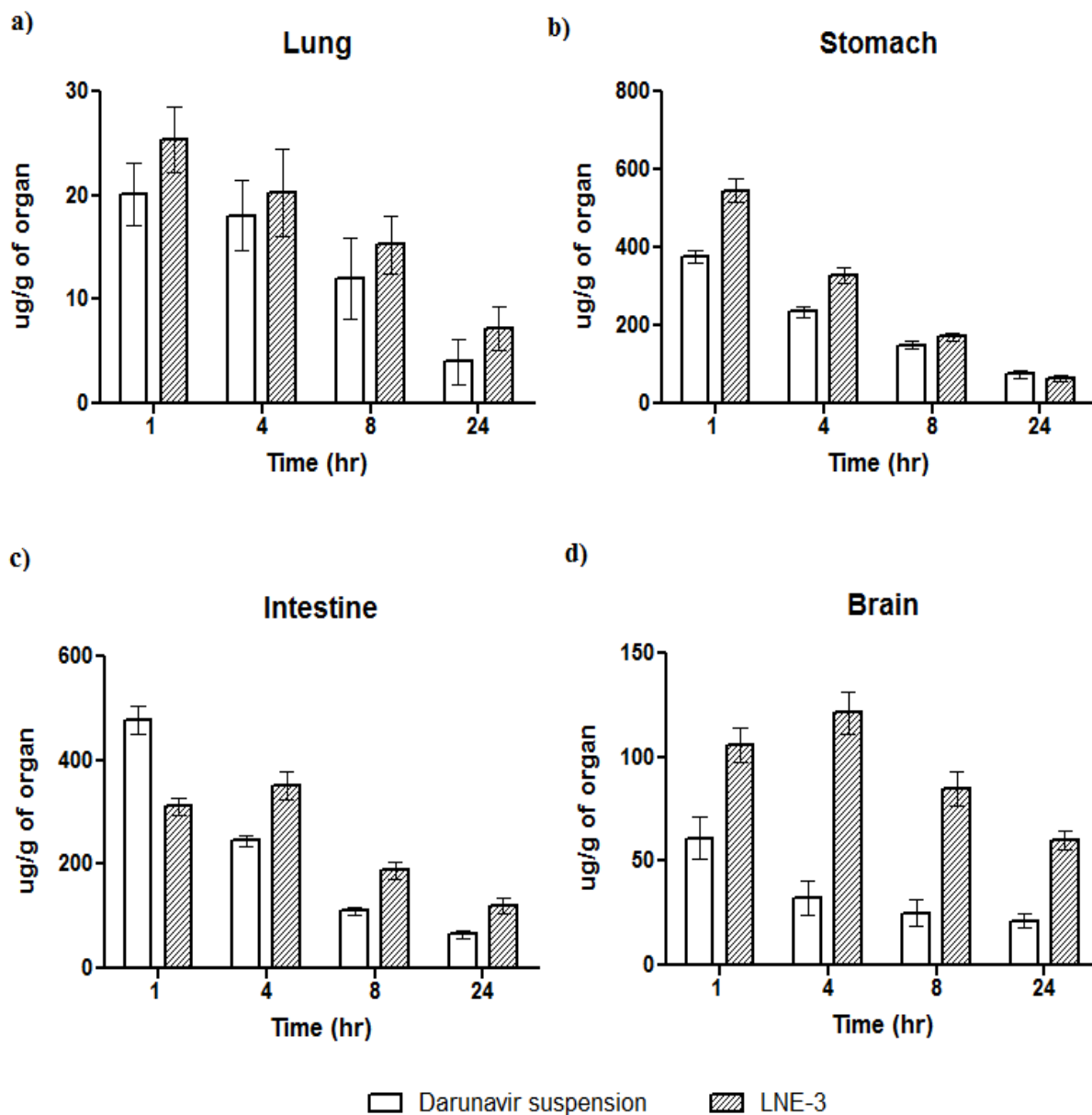


**Figure 7.18 Comparison of Darunavir concentration obtained in lung, stomach, intestine and brain upon administration of plain drug suspension and Darunavir loaded lipid nanoemulsion**

## 7.5.4 In-vivo methods of optimized Peptide grafted Atazanavir sulfate loaded SLNs

### 7.5.4.1 Pharmacokinetic study

Atazanavir sulfate loaded nanoparticles showed significant enhancement in the plasma drug profile in comparison to plain drug suspension (Table 7.15).  $C_{max}$  and  $AUC_{0-t}$  for ALN-23 increased by 2.71 and 2.12 fold in comparison to plain drug suspension (Table 7.16). Relative bioavailability for both the nanoparticle formulations increased by more than 200 % in comparison to plain ATZ suspension indicating the potential use of solid lipid carriers in bioavailability enhancement. Use of nanoparticles form increases the solubility of Atazanavir sulfate resulting in higher absorption rate as indicated by the decrease in  $T_{max}$  for ALN-23 (2 hr) in comparison to plain drug suspension (4 hr). The paired t-test suggested a nonsignificant difference in the plasma profiles of non-peptide grafted and peptide grafted ATZ nanoparticles. This indicates that the grafting of peptide on the nanoparticles surface lead to no significant change in its pharmacokinetic profile.

**Table 7.15 Plasma concentration vs time profile after oral administration of peptide grafted ATZ loaded SLNs (Pept-ATZ-SLN) and non-peptide grafted ATZ loaded SLNs (ALN-23) to rats (n=3)**

Time (hr)	Atazanavir sulfate concentration in plasma (ng/ml)		
	Pept-ATZ-SLN	ALN-23	ATZ suspension
0	0	0	0
0.5	118.7 ± 21.26	123.5 ± 20.47	22.7 ± 13.36
1	316.3 ± 44.44	323.2 ± 33.57	64.3 ± 32.36
2	767.9 ± 68.62	711.0 ± 88.45	116.4 ± 47.14
4	311.2 ± 50.36	322.3 ± 76.85	261.3 ± 49.35
8	61.4 ± 30.78	70.3 ± 23.25	43.4 ± 22.32
12	21.5 ± 12.53	10.3 ± 8.47	24.5 ± 13.26

\*Values are represented as mean ± SD, n=3

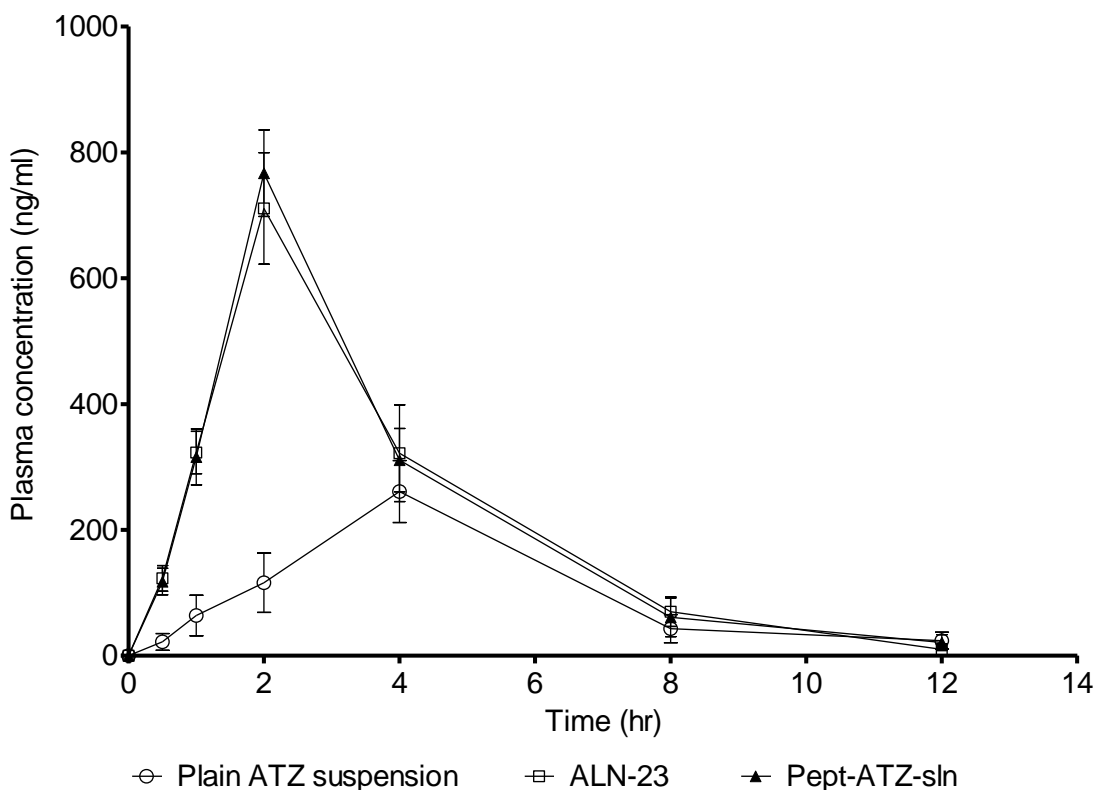


**Figure 7.19** Comparison of plasma concentration versus time profile after oral administration of plain ATZ suspension, ATZ loaded SLNs and peptide grafted ATZ loaded SLNs

**Table 7.16** Results of pharmacokinetic parameters upon oral administration of Atazanavir loaded SLNs and plain drug suspension to rats (n=3)

Parameter	Pept-ATZ-SLN	ALN-23	ATZ suspension
C <sub>max</sub> (ng/ml)	767.9 ± 68.62	711.0 ± 88.45	261.3 ± 49.35
T <sub>max</sub> (hr)	2	2	4
AUC <sub>0-t</sub> (ng.hr/ml)	2670.62±446.15	2639.35±508.57	1240.67 ± 365.3
AUC <sub>0-∞</sub> (ng.hr/ml)	2722.04±489.89	2666.16±533.99	1308.20 ± 419.14
T <sub>1/2</sub> (hr)	1.92 ± 0.25	1.65 ± 0.19	2.34 ± 0.29
MRT	3.50 ± 0.34	3.43 ± 0.22	5.01 ± 0.33
Relative bioavailability	215.25 %	212.73 %	-

\*Values are represented as mean ± SD, n=3

#### 7.5.4.2 Organ biodistribution study

Biodistribution pattern of Atazanavir in to different organs upon suspension, peptide grafted and non-peptide grafted nanoparticle administration was studied and the results are shown in Table 7.17, Table 7.18 and Table 7.19. The comparison of its distribution with the suspension form into various organs is depicted in Figure 7.20 and Figure 7.21. There was significant improvement ( $P < 0.05$ ) in tissue accumulation of Atazanavir into different organs upon SLN administration in comparison to plain drug suspension. There was significant difference ( $P < 0.05$ ) found between the drug concentrations in spleen and liver for peptide grafted and non-peptide grafted nanoparticles due to presence of T-cell binding peptide. In other organs, no statistical differences were observed between distributions of both the nanoparticles. Moreover, in comparison to plain drug suspension, nanoparticle formulations showed higher drug accumulation in spleen, heart, brain and lung which are considered as anatomical reservoirs sites for HIV (28).

**Table 7.17 Results of biodistribution study in different organs upon administration of ATZ suspension**

Time (hr)	ATZ concentration ( $\mu\text{g/g}$ of organ) in various organs upon administration of ATZ suspension							
	Liver	Spleen	Kidney	Heart	Lung	Stomach	Intestine	Brain
1	42.23 $\pm$ 8.17	9.17 $\pm$ 2.32	14.9 $\pm$ 6.32	2.86 $\pm$ 0.46	3.12 $\pm$ 0.87	25.43 $\pm$ 12.2	36.6 $\pm$ 12.21	2.35 $\pm$ 2.26
2	52.20 $\pm$ 7.62	16.5 $\pm$ 7.71	32.8 $\pm$ 7.74	2.36 $\pm$ 1.1	3.68 $\pm$ 1.45	56.8 $\pm$ 11.1	73.99 $\pm$ 9.27	4.67 $\pm$ 2.63
4	83.63 $\pm$ 9.9	36.63 $\pm$ 7.1	69.26 $\pm$ 10.27	5.07 $\pm$ 1.15	6.42 $\pm$ 1.26	108.23 $\pm$ 9.9	99.32 $\pm$ 7.71	13.25 $\pm$ 4.42
12	24.49 $\pm$ 5.34	12.25 $\pm$ 6.28	3.96 $\pm$ 2.2	0.28 $\pm$ 0.12	1.57 $\pm$ 0.76	7.53 $\pm$ 1.65	15.35 $\pm$ 6.6	2.88 $\pm$ 1.69

\*Values are represented as mean  $\pm$  SD, n=3

**Table 7.18 Results of biodistribution study in different organs upon administration of ATZ loaded SLNs**

Time (hr)	ATZ concentration ( $\mu\text{g/g}$ of organ) in various organs upon administration of ALN-23							
	Liver	Spleen	Kidney	Heart	Lung	Stomach	Intestine	Brain
1	40.32 $\pm$ 4.43	54.84 $\pm$ 13.32	13.89 $\pm$ 5.18	7.12 $\pm$ 0.84	5.61 $\pm$ 1.25	209.49 $\pm$ 17.67	88.03 $\pm$ 12.19	14.43 $\pm$ 3.59
2	51.14 $\pm$ 8.48	78.45 $\pm$ 11.21	23.64 $\pm$ 7.72	9.22 $\pm$ 1.13	11.79 $\pm$ 1.26	84.28 $\pm$ 13.28	157.66 $\pm$ 17.72	37.94 $\pm$ 5.58
4	31.85 $\pm$ 4.12	34.67 $\pm$ 10.1	54.92 $\pm$ 8.8	5.56 $\pm$ 1.15	3.47 $\pm$ 1.22	27.04 $\pm$ 8.93	65.23 $\pm$ 10.28	17.8 $\pm$ 4.16
12	20.63 $\pm$ 2.72	19.7 $\pm$ 6.21	10.11 $\pm$ 3.48	0.41 $\pm$ 0.11	3.11 $\pm$ 0.97	6.4 $\pm$ 2.12	41.7 $\pm$ 8.37	12.21 $\pm$ 3.32

\*Values are represented as mean  $\pm$  SD, n=3**Table 7.19 Results of biodistribution study in different organs upon administration of peptide grafted ATZ loaded SLNs**

Time (hr)	ATZ concentration ( $\mu\text{g/g}$ of organ) in various organs upon administration of pept-ATZ-SLN							
	Liver	Spleen	Kidney	Heart	Lung	Stomach	Intestine	Brain
1	33.85 $\pm$ 5.32	98.39 $\pm$ 15.61	13.47 $\pm$ 4.6	7.49 $\pm$ 0.73	4.78 $\pm$ 1.0	200.48 $\pm$ 11.9	86.38 $\pm$ 10.1	15.1 $\pm$ 3.11
2	40.69 $\pm$ 7.7	131.6 $\pm$ 10.28	21.88 $\pm$ 7.26	8.37 $\pm$ 1.16	12.38 $\pm$ 1.17	74.82 $\pm$ 8.27	152.38 $\pm$ 15.24	36.65 $\pm$ 4.32
4	27.4 $\pm$ 4.41	74.38 $\pm$ 7.82	55.49 $\pm$ 9.1	5.45 $\pm$ 0.92	3.15 $\pm$ 1.19	25.39 $\pm$ 5.55	63.29 $\pm$ 8.82	17.39 $\pm$ 2.37
12	14.39 $\pm$ 4.12	36.8 $\pm$ 5.36	9.4 $\pm$ 3.12	0.37 $\pm$ 0.13	3.04 $\pm$ 1.11	4.81 $\pm$ 0.87	40.89 $\pm$ 5.52	11.8 $\pm$ 2.12

\*Values are represented as mean  $\pm$  SD, n=3

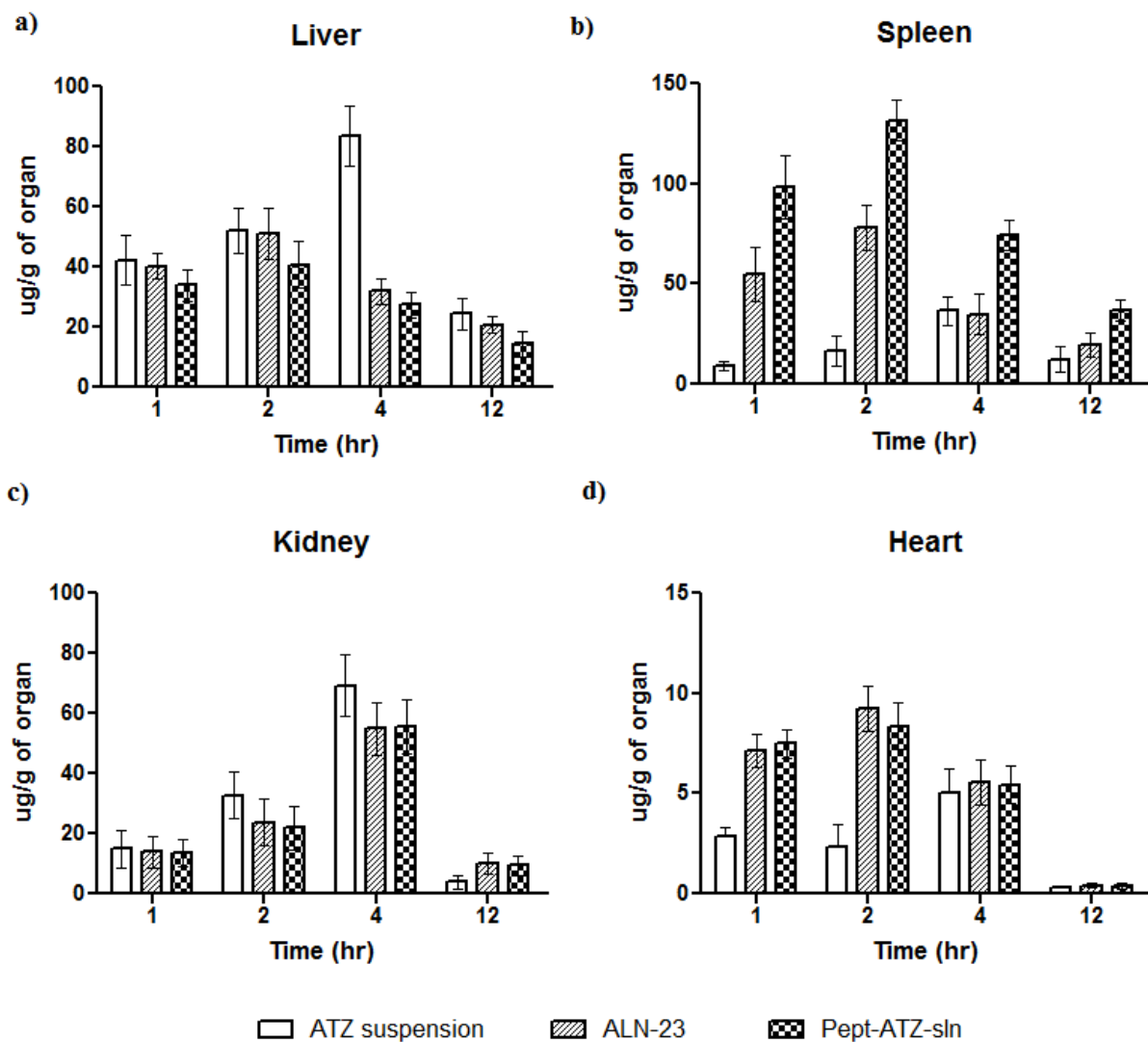


**Figure 7.20 Comparison of ATZ concentration obtained in liver, spleen, kidney, and heart upon administration of ATZ suspension, ATZ loaded SLNs and peptide grafted ATZ loaded SLNs**

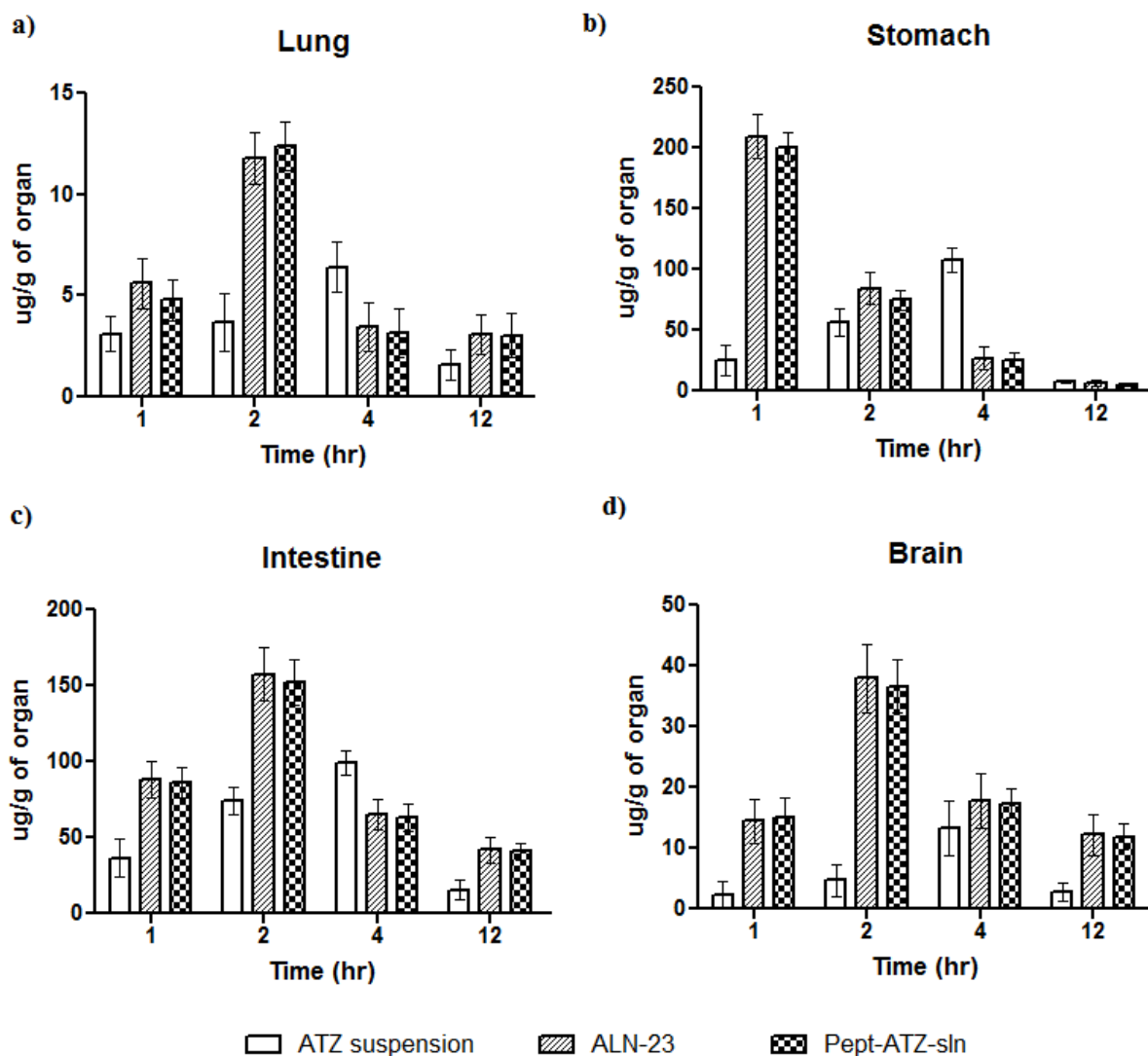


**Figure 7.21 Comparison of ATZ concentration obtained in liver, spleen, kidney, and heart upon administration of ATZ suspension, ATZ loaded SLNs and peptide grafted ATZ loaded SLNs**

## 7.6 References

1. CDER U. Guidance for Industry: Estimating the maximum safe starting dose in initial clinical trials for therapeutics in adult healthy volunteers. US Department of Health and Human Services Food and Drug Administration Center for Drug Evaluation and Research. 2005.
2. Thommes M, Baert L, van't Klooster G, Geldof M, Schueller L, Rosier J, et al. Improved bioavailability of darunavir by use of  $\kappa$ -carrageenan versus

- microcrystalline cellulose as pelletisation aid. *Eur J Pharm Biopharm.* 2009;72(3):614-20.
3. Li H, Zhao X, Ma Y, Zhai G, Li L, Lou H. Enhancement of gastrointestinal absorption of quercetin by solid lipid nanoparticles. *Journal of Controlled Release.* 2009;133(3):238-44.
  4. McConnell EL, Basit AW, Murdan S. Measurements of rat and mouse gastrointestinal pH, fluid and lymphoid tissue, and implications for in-vivo experiments. *Journal of Pharmacy and Pharmacology.* 2008;60(1):63-70.
  5. Desai MP, Labhsetwar V, Amidon GL, Levy RJ. Gastrointestinal uptake of biodegradable microparticles: effect of particle size. *Pharm Res.* 1996 Dec;13(12):1838-45.
  6. Nebendahl K. Routes of administration. *The laboratory rat San Diego (CA): Academic Press p.* 2000:463-83.
  7. Fukushima K, Terasaka S, Haraya K, Kodera S, Seki Y, Wada A, et al. Pharmaceutical approach to HIV protease inhibitor atazanavir for bioavailability enhancement based on solid dispersion system. *Biological and Pharmaceutical Bulletin.* 2007;30(4):733-8.
  8. Singh G, Pai RS. Atazanavir-loaded Eudragit RL 100 nanoparticles to improve oral bioavailability: optimization and in vitro/in vivo appraisal. *Drug delivery.* 2014 (0):1-8.
  9. Aji Alex MR, Chacko AJ, Jose S, Souto EB. Lopinavir loaded solid lipid nanoparticles (SLN) for intestinal lymphatic targeting. *European journal of pharmaceutical sciences : official journal of the European Federation for Pharmaceutical Sciences.* 2011;42(1-2):11-8.
  10. Chakraborty S, Shukla D, Mishra B, Singh S. Lipid--an emerging platform for oral delivery of drugs with poor bioavailability. *Eur J Pharm Biopharm.* 2009 Sep;73(1):1-15.
  11. Zhang Z, Gao F, Bu H, Xiao J, Li Y. Solid lipid nanoparticles loading candesartan cilexetil enhance oral bioavailability: in vitro characteristics and absorption mechanism in rats. *Nanomedicine.* 2012 Jul;8(5):740-7.

12. Wong HL, Chattopadhyay N, Wu XY, Bendayan R. Nanotechnology applications for improved delivery of antiretroviral drugs to the brain. *Advanced drug delivery reviews*. 2010;62(4):503-17.
13. Kaur A, Jain S, Tiwary A. Mannan-coated gelatin nanoparticles for sustained and targeted delivery of didanosine: in vitro and in vivo evaluation. *Acta pharmaceutica*. 2008;58(1):61-74.
14. Kreuter J. Nanoparticulate systems for brain delivery of drugs. *Advanced drug delivery reviews*. 2001;47(1):65-81.
15. Ahsan F, Rivas IP, Khan MA, Suarez AIT. Targeting to macrophages: role of physicochemical properties of particulate carriers—liposomes and microspheres—on the phagocytosis by macrophages. *Journal of controlled release*. 2002;79(1):29-40.
16. Cornes J. Number, size, and distribution of Peyer's patches in the human small intestine: Part I The development of Peyer's patches. *Gut*. 1965;6(3):225.
17. Eldridge JH, Hammond CJ, Meulbroek JA, Staas JK, Gilley RM, Tice TR. Controlled vaccine release in the gut-associated lymphoid tissues. I. Orally administered biodegradable microspheres target the Peyer's patches. *Journal of Controlled Release*. 1990;11(1):205-14.
18. Ebel JP. A method for quantifying particle absorption from the small intestine of the mouse. *Pharmaceutical research*. 1990;7(8):848-51.
19. O'Hagan D, Palin K, Davis S. Intestinal absorption of proteins and macromolecules and the immunological response. *Critical reviews in therapeutic drug carrier systems*. 1987;4(3):197-220.
20. Collnot E-M, Baldes C, Wempe MF, Kappl R, Hüttermann J, Hyatt JA, et al. Mechanism of inhibition of P-glycoprotein mediated efflux by vitamin E TPGS: influence on ATPase activity and membrane fluidity. *Molecular pharmaceutics*. 2007;4(3):465-74.
21. Rao Z, Si L, Guan Y, Pan H, Qiu J, Li G. Inhibitive effect of cremophor RH40 or tween 80-based self-microemulsifying drug delivery system on cytochrome P450 3A enzymes in murine hepatocytes. *Journal of Huazhong University of Science and Technology [Medical Sciences]*. 2010;30:562-8.

22. Caliph SM, Charman WN, Porter CJ. Effect of short-, medium-, and long-chain fatty acid-based vehicles on the absolute oral bioavailability and intestinal lymphatic transport of halofantrine and assessment of mass balance in lymph-cannulated and non-cannulated rats. *Journal of pharmaceutical sciences*. 2000;89(8):1073-84.
23. Jiang ZM, Zhang S, Wang X, Yang N, Zhu Y, Wilmore D. A comparison of medium-chain and long-chain triglycerides in surgical patients. *Annals of surgery*. 1993;217(2):175.
24. Porter CJ, Pouton CW, Cuine JF, Charman WN. Enhancing intestinal drug solubilisation using lipid-based delivery systems. *Advanced Drug Delivery Reviews*. 2008;60(6):673-91.
25. Prabhakar K, Afzal SM, Surender G, Kishan V. Tween 80 containing lipid nanoemulsions for delivery of indinavir to brain. *Acta Pharmaceutica Sinica B*. 2013;3(5):345-53.
26. Zara GP, Cavalli R, Bargoni A, Fundarò A, Vighetto D, Gasco MR. Intravenous administration to rabbits of non-stealth and stealth doxorubicin-loaded solid lipid nanoparticles at increasing concentrations of stealth agent: pharmacokinetics and distribution of doxorubicin in brain and other tissues. *Journal of drug targeting*. 2002;10(4):327-35.
27. Kreuter J. Influence of the surface properties on nanoparticle-mediated transport of drugs to the brain. *Journal of nanoscience and nanotechnology*. 2004;4(5):484-8.
28. das Neves J, Amiji MM, Bahia MF, Sarmiento B. Nanotechnology-based systems for the treatment and prevention of HIV/AIDS. *Adv Drug Deliv Rev*. 2010 Mar 18;62(4-5):458-77.